



Remak, Sarah-Jane (2021) *Targeting the RON-MSP axis and harnessing antitumour $\gamma\delta$ T cells to counteract breast cancer metastasis*. MSc(R) thesis.

<https://theses.gla.ac.uk/82494/>

Copyright and moral rights for this work are retained by the author

A copy can be downloaded for personal non-commercial research or study, without prior permission or charge

This work cannot be reproduced or quoted extensively from without first obtaining permission in writing from the author

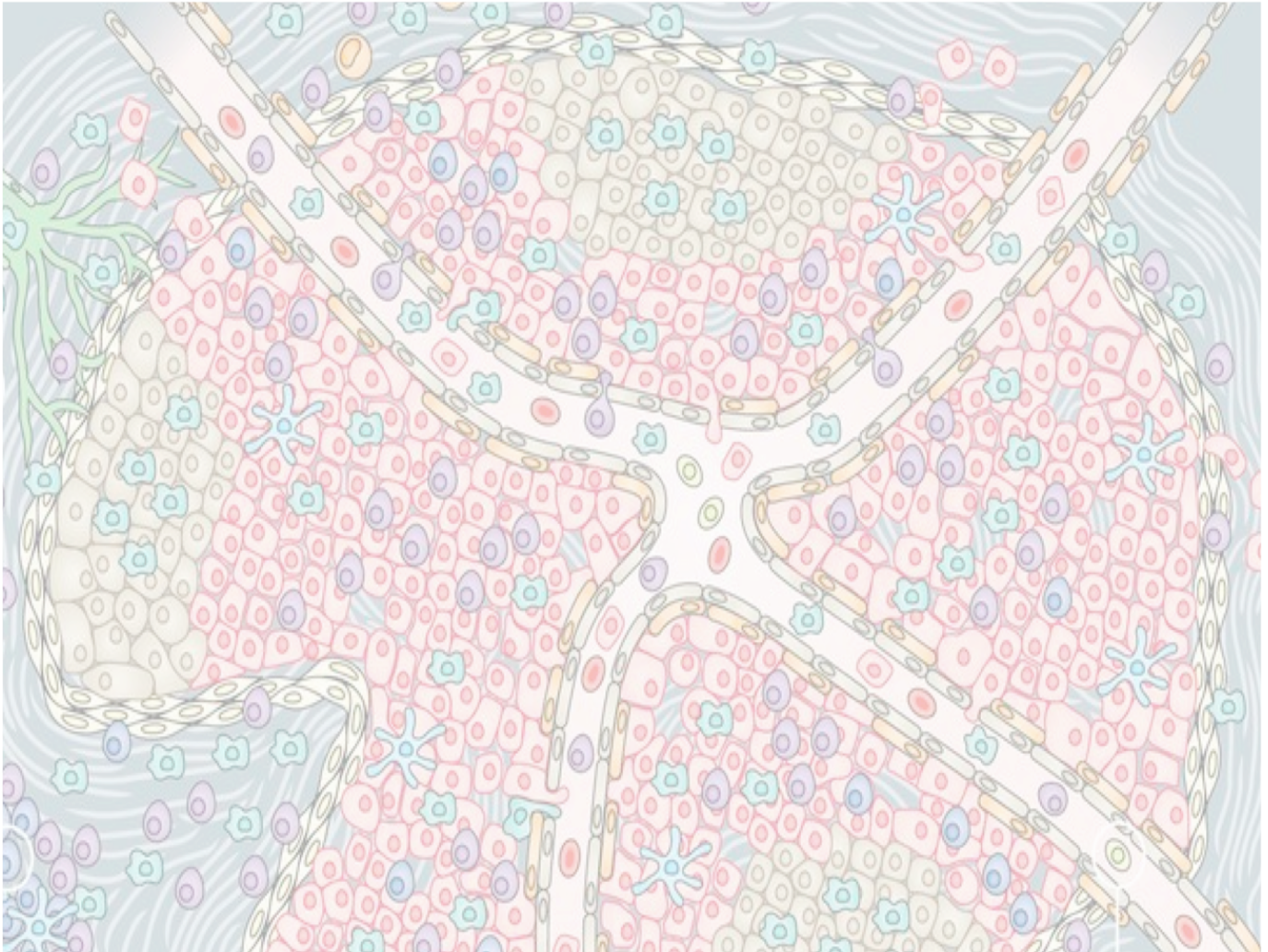
The content must not be changed in any way or sold commercially in any format or medium without the formal permission of the author

When referring to this work, full bibliographic details including the author, title, awarding institution and date of the thesis must be given

Enlighten: Theses

<https://theses.gla.ac.uk/>
research-enlighten@glasgow.ac.uk

Targeting the RON-MSP axis and harnessing anti-tumour $\gamma\delta$ T cells to counteract breast cancer metastasis



Sarah-Jane Remak

MSc Cancer Sciences

Supervisors: Dr. Seth Coffelt & Dr. Karen Blyth

June 2021

Table of contents

Chapter I. Introduction	5
1.1 Molecular breast cancer subtypes	5
1.1.1. Luminal A/B and normal-like.....	5
1.1.2. HER2-amplified	6
1.1.3. Basal-like and/or triple-negative	6
1.2 BRCA1-deficient breast cancer	7
1.2.1 BRCA1	7
1.3 Metastasis	8
1.3.1. Immune cells in the tumour microenvironment	9
1.3.1.1. Macrophages	10
1.3.1.2. Neutrophils	11
1.3.1.3 $\gamma\delta$ T cells.....	11
1.4 Rationale	13
1.4.1. $\gamma\delta$ T cell - IL-17 - neutrophil metastatic cascade in breast cancer	13
1.4.2 BRCA1-deficient cancer model	16
1.4.3. RON-MSP axis in breast cancer metastasis	18
Chapter II. Materials and methods	23
2.1 Mice and animal experiments.....	23
2.2 Generation of primary mouse breast cancer cell lines and cell culture.....	24
2.3 Western blotting.....	25
2.4 Immunohistochemistry	26
2.5 ELISA.....	26
2.6 Cell viability assay - crystal violet	27
2.7 Flow cytometry - surface and intracellular staining.....	27
2.8 Real-time cytotoxicity assay.....	30
2.9 Invasion assay	30
2.10 Statistical analysis.....	31

Chapter III. Results	32
3.1 BRCA1-deficient mice show neutrophilia and IL-17-producing $\gamma\delta$ T cells are increased in BRCA1-deficient mice	32
3.2 MSP expression, but not RON expression is increased in mammary tumours of BRCA1-deficient mice	35
3.3 MSP overexpression does not alter macrophage polarisation in BRCA1-deficient mice and neutrophil infiltration is absent in BRCA1-deficient mammary tumours.....	37
3.4 BRCA1-deficient tumour cells secrete MSP to activate the RON-MSP axis	40
3.5 Inhibition of RON by BMS-777607 does not reduce cell viability in BRCA1-deficient cancer cell lines	42
3.6 The RON-MSP axis plays a role in the invasiveness of BRCA1-deficient tumour cells	45
3.7 The $V\gamma 1$ $\gamma\delta$ T cell subset is restricted to IFNγ-producing $\gamma\delta$ T cells and $V\gamma 4$ $\gamma\delta$ T cells expand in the presence of a mammary tumour	47
3.8 Anti-$V\gamma 1$ antibody selectively depletes IFNγ-producing $\gamma\delta$ T cells and decreases IFNγ production on CD3⁺ T cells	48
 Chapter IV. Discussion	 52
 Chapter V. References.....	 57

Abstract

Breast cancer metastasis accounts for 90% of breast cancer-related deaths. Triple-negative breast cancer (TNBC) is the most aggressive breast cancer subtype and associated with the poorest prognosis, limited treatment options and high relapse rates. Therefore, exploiting new targets to abrogate metastasis are required. We show that mammary tumours from *K14Cre;Brca1^{F/F};Trp53^{F/F}* (KB1P) mice, a mouse of model TNBC, have elevated expression of macrophage-stimulation protein (MSP), the ligand of the tyrosine kinase receptor Recepteur d'origine nantais (RON). Using cell lines derived from KB1P mammary tumours, we observed that endogenous MSP promotes invasiveness *in vitro*, which can be pharmacologically abrogated by a RON inhibitor. The role of the cancer cell-initiated $\gamma\delta$ T cell - IL-17 - neutrophil axis in breast cancer metastasis has been demonstrated in a mouse model of lobular breast cancer. We observed that this metastatic cascade is also relevant in KB1P mice. In contrast to their IL-17 producing counterparts, IFN γ $\gamma\delta$ T cells are implied to have anti-tumourigenic potential, but their role in breast cancer metastasis remains elusive. We found that expression of the V γ 1 variant of the T-cell receptor (TCR) is specific to IFN γ $\gamma\delta$ T cells. Successful depletion of these cells with an anti- V γ 1 antibody was accompanied with a reduction of IFN γ expression on CD3+ T cells. Our long-term goal is to combine $\gamma\delta$ T cell immunotherapy with other targeted anti-cancer therapies. Here, we describe the RON-MSP as viable target for breast cancer treatment and provide initial evidence for a protective anti-tumourigenic role of IFN γ $\gamma\delta$ T cells in breast cancer metastasis by priming CD8⁺ T cells to exert their cytotoxic function.

Chapter I. Introduction

1.1 Molecular breast cancer subtypes

Breast cancer is the second most commonly diagnosed type of cancer worldwide and the leading cause of cancer-related deaths in women [1]. The heterogeneity of breast cancer is well known and arises from the transformation of different mammary cell types. This results in a heterogeneous group of cancers with differences in clinical implication, histopathology and a response to therapy. Clinically, breast cancer is classified based on tumour grade, tumour stage, and expression of the hormone receptors progesterone (PR), oestrogen (ER) and/or the epidermal human epidermal growth factor receptor 2 (HER2), as determined by immunohistochemistry [2]. This classification has limitations in predicting the prognosis of cancer patients as advances in gene expression analysis have shown that the response to cancer treatment is determined by molecular characteristics of the cancer cells and not by anatomical pathology of the tumour [3]. Based on the gene expression profile, at least five molecular breast cancer subtypes can be classified: luminal A, luminal B, HER2 (ERBB2-)-amplified, normal breast-like and basal-like [4]. This molecular classification has clinical relevance as a prognostic marker and to identify the most effective treatment for the patient [5].

1.1.1. Luminal A/B and normal-like

The majority (~70-80%) of breast cancer tumours are of the luminal A/B subtype.

These tumours express hormone receptors PR and/or ER and are therefore sensitive to hormone therapy using tamoxifen, the most commonly used drug for luminal tumours [6]. Luminal A breast cancer is HER2 negative and has low levels of the cell proliferation marker Ki-67 [7]. In contrast, luminal B breast cancer tumours are HER2 positive (20%) or negative and show higher levels of Ki-67, resulting in a slightly

worse prognosis than luminal A breast cancer tumours, which grow more slowly and generally have a better prognosis [7, 8]. Normal-like breast tumours have not been well defined, but show characteristics similar to luminal A, albeit with a worse prognosis [9].

1.1.2. HER2-amplified

Of all breast cancer tumours, 10-20% show amplification of the HER2 (ERBB2) oncogene and are negative for hormone receptors ER and PR. HER2 is a receptor tyrosine kinase involved in signalling pathways that regulate cell growth, migration and differentiation, apoptosis and cell motility [10]. HER2-amplified breast tumours have a worse prognosis than luminal cancers and are highly proliferative and aggressive. These tumours are sensitive to chemotherapy and this is the first line of treatment in combination with targeted therapies against the HER2 protein, such as Trastuzumab and Lapatinib [11].

1.1.3. Basal-like and/or triple-negative

Basal-like breast cancers represent 10-20% of all breast tumours. This subtype of breast tumours is commonly referred to as triple-negative breast cancer (TNBC). While approximately 80% of TNBC tumours show a basal-like phenotype, TNBC and basal-like breast cancer are not synonymous and terms should not be used interchangeably [12]. TNBCs are defined by negative immunohistochemistry staining for PR, ER and HER2. In contrast, a clear definition of the 'basal-like phenotype' remains elusive (reviewed in [13]) Generally, basal-like breast cancer (BLBC) tumours are characterised by expression of basal cytokeratins (i.e. CK5/6, CK14 and/or CK17) and luminal cytokeratins (i.e. CK8/18 and/or CK19). Interestingly, this suggests that basal-like tumours are not derived from a single stem cell type. It should be noted that the most consistent expression amongst basal-like tumours was found for basal

CK5/6 and luminal CK8/18 [14, 15]. Furthermore, there are other markers that have been assigned to the basal-like phenotype. These include, but are not limited to: vimentin and laminin, which are both involved in maintaining the integrity of the extracellular matrix, and p63 (reviewed in [13]). Basal-like tumours are associated with an aggressive phenotype, highly proliferative and invasive tumours and are insensitive to targeted therapies used for luminal and HER2-amplified tumours because they are generally PR/ER/HER2-negative.

1.2 BRCA1-deficient breast cancer

Extensive evidence has suggested a link between sporadic basal-like breast cancer (BLBC) and familial *BRCA1*-mutant tumours. Indeed, over 75% of *BRCA1*-mutated breast tumours showed a basal-like phenotype [15]. Both BLBCs and *BRCA1*-mutated tumours are often triple-negative and show a high frequency of mutations in the *TP53* gene [16]. Germline mutations in *BRCA1* (or *BRCA2*) are associated with a significantly increased risk of breast (70-80%) and ovarian cancer (50-60%) and to a lesser extent, other cancers [17].

1.2.1 BRCA1

Although multiple mechanisms have been suggested to explain how *BRCA1* mutations cause cancer, the role of BRCA1 in DNA repair has been studied most extensively. BRCA1 binds to multiple proteins to form protein complexes, such as BRCA2 and RAD51, to repair double-strand DNA breaks (DSBs) by means of homologous recombination (HR) [16]. This is a sophisticated mechanism to repair DNA and restore the DNA sequence to its original form. When BRCA1 function is impaired, for example when BRCA1 is mutated, HR is absent and DSBs are repaired by non-homologous end joining (NHEJ) [18]. DNA repair by NHEJ combines the two broken DNA strands together without a homologous DNA sequence as a guide

sequence [19]. Therefore, NHEJ is prone to the introduction of DNA mutations, which most commonly results in DNA deletions [19]. Thus, *BRCA1*-mutated tumours show extreme genomic instability. Indeed, these tumours are highly sensitive to agents that interfere with DNA replication, such as PARP inhibitors and platinum salts (e.g. cisplatin). These drugs exploit the impaired DNA repair by HR. More specifically, cells either fail to repair the drug-induced DNA damage, which programs the cell to undergo cell death (apoptosis), or the genomic instability induced by error-prone NHEJ renders cells to become non-viable [19].

In addition to germline mutations in *BRCA1*, it is now widely recognised that sporadic breast tumours with defects in genes involved in HR can show a similar phenotype (i.e. BRCAness) to tumours with a germline *BRCA1* mutation [20]. Moreover, recent studies have shown that other cancers, including prostate cancer and pancreatic cancers can also exhibit BRCAness. This has clinical significance, as this suggests that tumours with this phenotype may also be sensitive to PARP inhibitors and platinum salts, such as cisplatin [21, 22].

1.3 Metastasis

Early screening and chemotherapy have significantly improved disease-free survival of breast cancer patients. Unfortunately, there has been little improvement in survival for breast cancer patients with metastatic disease. Metastasis accounts for 90% of breast cancer-related deaths and less than 25% of patients with metastatic disease live beyond five years [23]. Basal-like breast cancer has the worst prognosis of all breast cancer types. Not only are treatment options limited, patients with basal-like breast cancer frequently show early relapse following chemotherapy due to the highly proliferative and invasiveness of the tumours [24].

Breast cancer most commonly metastasises to the bone, lung, liver, brain and lymph nodes [25], indicating that metastasis is not a random process. Indeed, metastasis is a multi-step process and starts with invasion of the surrounding tissue. In order to escape from the primary tumour site, the tumour cells must remodel their cell-matrix and cell-cell adhesion interactions to acquire invasive properties. Subsequently, the tumours enter the blood vessels and/or lymphatic vessels and travel to distant organs. At the metastatic site(s) the tumours cells adhere to the capillary beds of the organs and extravasate into the organ. Once embedded, the tumours cells proliferate and promote angiogenesis to form the metastatic tumour [26]. Importantly, abrogation of any step in this 'metastatic cascade' arrests the metastatic process. Indeed, the rate-limiting steps for metastasis are proposed to be tumour cell extravasation and metastatic growth [27].

1.3.1. Immune cells in the tumour microenvironment

It is now well established that the inflammatory tumour microenvironment (TME) has a very important role in metastasis (and primary tumour growth) [28]. Although mutations in tumour suppressor genes and/or oncogenes drive the malignancy of cancer cells, the tumour microenvironment evolves with the cancer cells and promotes cancer progression and metastatic disease. Immune cells, including macrophages, neutrophils and gamma-delta T cells are recruited to the tumour microenvironment and exhibit pro-tumourigenic functions [29, 30] to aid tumour progression.

1.3.1.1. Macrophages

Macrophages are innate immune cells and their physiological function is to defend against pathogens and maintain tissue homeostasis. There is strong evidence that macrophages play a pivotal role in tumour initiation and progression and are involved in therapy resistance seen in cancer patients [31]. Indeed, in breast cancer, macrophages are the most abundant cells in the TME and can make up over 50% of the total tumour mass [32]. Moreover, in humans, macrophage density in the tumour is associated with worse prognosis and increases the likelihood of metastasis and reoccurrence of the primary tumour [33]. Tumour-associated macrophages (TAMs) in the breast tumour originate from resident macrophages and circulating monocytes, which are recruited to the TME where they develop into non-polarised macrophages. Macrophages show high levels of plasticity and can change their phenotype depending on immune context and environmental signals (e.g. cytokines). Classically, these TAM populations were classed into M1 and M2 macrophage subtypes [34, 35]. M1-like macrophages have anti-tumour capacity by secreting pro-inflammatory cytokines, while M2-like macrophages have pro-tumour characteristics. It is now well recognised that these are the two extremes on a continuous spectrum and that monocytes can develop into different macrophage subtypes based on the molecular markers they express [36]. TAMs in the tumour microenvironment are closely related to the M2-like macrophage subtype and promote tumour growth by affecting immune suppression, angiogenesis, invasion and metastasis [37, 38]. More specifically, using an MMTV-PyMT mouse model, Lin and Pollard have demonstrated that TAMs at the primary tumour site are important for suppressing CD8-T cell [39] and NK cell function to protect the tumour cells from the immune system (reviewed in [40]). Metastasis-associated macrophages, a

population different from TAMs, prime the metastatic site (before arrival of tumour cells) and also stimulate extravasation of the tumour cells by secretion of VEGF and promote their survival and growth at the distant site, for example by secreting CSF-1 [40, 41]. Furthermore, several studies using breast cancer xenograft mouse models have also suggested that TAMs induce resistance in treatment [42, 43].

1.3.1.2. Neutrophils

Neutrophils are another type of innate immune cell, which make up 50-70% of all leukocytes and are the most abundant immune cell population in humans [44].

Patients with various cancers, including lung and breast cancer, show an increased number of neutrophils in the blood, which is correlated to worse survival in patients [45, 46]. While it has been known that neutrophils are present in the tumour microenvironment, recently, they have gained more attention. Several studies have shown that neutrophils change their phenotype to promote tumour initiation, progression and metastasis. Moreover, neutrophils can manipulate the function of other immune cells in the TME to facilitate cancer progression and metastasis (reviewed in [47]).

1.3.1.3 $\gamma\delta$ T cells

Gamma-delta ($\gamma\delta$) T cells are a subset of T cells and represent 0.5-5% of all T-lymphocytes in humans. They are composed of a γ chain and a δ chain of the T cell receptor (TCR) and are involved in immune responses, responses to infection and tissue damage and are implicated in autoimmune diseases [48]. In the peripheral blood, $\gamma\delta$ T cells account for 5% of all CD3⁺ T-cells. The vast majority, approximately 95%, of T cells in the peripheral blood, are $\alpha\beta$ T cells, which have a TCR made up of

α and β chains [49]. These $\alpha\beta$ T cells generally express CD4 and CD8 lineage markers and require antigen presentation through recognition by major histocompatibility complex (MHC) molecules [50]. Although they have a TCR, unlike $\alpha\beta$ T cells, $\gamma\delta$ T cells are not restricted to antigen recognition by MHC and recognise a variety of stress-induced molecules, metabolites and pathogen-associated peptides [51, 52]. They have the ability to secrete a variety of cytokines, including but not limited to, interferon- γ (IFN γ) and interleukin-17 (IL-17). Furthermore, they also express natural killer receptors (e.g. NKG2D) and exert a rapid immune response upon stimulation in the periphery [49, 53]. Consequently, $\gamma\delta$ T cells are proposed to be involved the first line of defence and considered to represent the bridge between the innate and adaptive immune system. $\gamma\delta$ T cells constitute of a heterogeneous population of cells and their function is linked with their tissue localisation [54]. Indeed, in mice, $\gamma\delta$ T cells subsets can be categorised based on the usage of the TCR γ -chain variable region (a similar distinction can be made in humans based on the δ -chain variable). These subsets have different effector functions, such as IFN γ and IL-17 production [55]. In mice, expression of the surface marker CD27 is restricted to IFN γ producing $\gamma\delta$ T cells [56]. Thus, CD27 can be used to distinguish between IFN γ $\gamma\delta$ T cells and IL-17 $\gamma\delta$ T cells. Various studies in mouse cancer models have shown that $\gamma\delta$ T cells can promote tumourigenesis. IL-17-producing $\gamma\delta$ T cells are one of the major sources of IL-17 in the tumour microenvironment [57] and can promote cancer development by promoting angiogenesis. Furthermore, several studies have shown that $\gamma\delta$ T cells can increase the population of myeloid derived suppressor cells (MDSCs), such as neutrophils. These cells are involved in promoting the immunosuppressive tumour

microenvironment and facilitate tumourigenesis in several types of cancer, including breast cancer.

1.4 Rationale

1.4.1. $\gamma\delta$ T cell - IL-17 - neutrophil metastatic cascade in breast cancer

Increased neutrophil abundance in breast cancer patients predicts a worsened metastasis-specific survival. However, the role of neutrophils in metastasis remains unclear, as both anti-metastatic and pro-metastatic functions have been described. Coffelt and colleagues investigated the role of neutrophils in metastasis using a conditional mouse model of lobular breast cancer [58]. This model has been described previously [59]. Briefly, the mouse tumour model is based on the knockout of epithelial-specific *P53* combined with conditional E-cadherin mutations, as human invasive lobular carcinomas frequently show a loss of E-cadherin, which is associated with tumour metastasis. These K14-cre;*Cdh1*^{F/F};*Trp53*^{F/F} (KEP) mice spontaneously develop invasive and metastatic mammary carcinomas that strongly resemble the human invasive lobular carcinomas. The role of neutrophils was also assessed using a KEP-based spontaneous breast cancer metastasis model, as described here [60]. KEP mice showed neutrophil expansion in various tissues, including the lungs, lymph nodes, liver, kidney, spleen, the (primary) tumour, and the blood. Similarly to the KEP mice, neutrophils also accumulated in these organs in the metastasis model. Quantification of the neutrophils showed that the number of neutrophils increased with tumour size. Moreover, removal of the primary tumour reduced neutrophil accumulation, supporting the fact that neutrophil expansion is tumour-induced. In order to determine whether neutrophils affected primary tumour growth and/or metastasis, neutrophils were depleted in the metastasis model with an anti-Ly6G

antibody. Interestingly, neutrophil depletion did not affect primary tumour growth, but resulted in a significant decrease in lymph node and lung metastases. Selective depletion of neutrophils in the early phase (onset of the primary tumour) or late phase (after surgical removal of the primary tumour) only showed a reduction in metastasis in the early phase, which implies a critical role of neutrophils in the early stage of the multi-step metastatic cascade. The circulating neutrophils were found to express high levels of cKIT, a hematopoietic stem cell marker commonly found on pro-metastatic myeloid cells, including immature neutrophils [58]. In order to decipher the mechanism of neutrophil-induced promotion of metastasis, RNA sequencing was performed. Data showed a 150-fold upregulation of *Nos2* gene that encodes inducible nitric oxide synthase (iNOS). Considering the fact that iNOS is associated with suppression of T cells [58], it was hypothesised that neutrophils promote metastasis by immunosuppression. When comparing the proliferation of naïve splenic CD8⁺ T cells *ex vivo* in the presence of neutrophils from tumour-bearing KEP mice or wild-type (WT) mice neutrophils, it was observed that CD3/CD28-induced proliferation was inhibited. In order to determine whether this was dependent on iNOS, an iNOS inhibitor was used. Interestingly, while depletion of iNOS reversed this effect, the proportions of the CD8⁺ T cells remained the same. More specifically, a phenotypic change was observed; depletion of the neutrophils by targeting iNOS enhanced the effector phenotype (expressed as CD62L⁻CD44⁺IFN γ ⁺ cells). Moreover, the metastasis phenotype was restored when both neutrophils and CD8⁺ T cells were depleted, which further supports a link between neutrophils and CD8⁺ T cell activity. To elucidate the link between expansion of the neutrophils and the mammary tumour (and its environment), cytokine profiling on the WT mammary glands and the KEP mammary tumours was performed. GM-CSF

and G-CSF play pivotal roles in neutrophil biology, but were not increased in the KEP mammary tumours. In contrast, cytokines that are known to stimulate IL-17 showed increased expression. It was hypothesised that IL-17 induced neutrophil expansion through G-CSF. Indeed, results showed that IL-17-G-CSF signalling was required for neutrophil expansion and their immunosuppressive phenotype. To determine the source of IL17 and with the knowledge that T cells are known to produce IL17, a T cell-specific gene expression array was utilised to analyse the CD3⁺ T cells of the spleen. Indeed, IL-17-related cytokines were increased in the splenic CD3⁺ T cells from KEP tumour bearing mice. To rule out the contribution of other immune cell populations to the observed upregulated IL-17 levels, KEP mice were crossed with *Rag1*^{-/-} mice, which lack T and B cells. The neutrophils (and their phenotype) and serum levels of IL17A and G-CSF in KEP;*Rag1*^{+/-} (control) and KEP;*Rag1*^{-/-} mice were investigated. Serum levels were lower in KEP;*Rag1*^{-/-} mice. Additionally, neutrophil counts were diminished, and their phenotype was altered. These data support that CD3⁺ T cells are the main source of IL-17. Moreover, KEP;*Rag1*^{-/-} mice also showed fewer lung and lymph node metastases. In summary, not only are lymphocytes the source of IL-17, these IL-17 producing lymphocytes also promote metastasis by driving neutrophil expansion and altering their phenotype.

Further experiments to determine what T cell subset is producing IL-17 showed that IL-17-producing $\gamma\delta$ T cells promote neutrophil expansion and support their immunosuppressive phenotype. These IL17-producing $\gamma\delta$ T cells were classified as CD27⁺V γ 4⁺. The pro-metastatic role of this $\gamma\delta$ T cell subset was also confirmed by using *Tcr δ* ^{-/-} mice, which lack $\gamma\delta$ T cells. Lastly, the initial steps were made to decipher the link between the mammary tumour and the $\gamma\delta$ T cells. It was found that IL-1 β secretion from the mammary tumour activated the IL-17-producing $\gamma\delta$ T cells

and macrophages were found to be the main source of IL-1 β . In summary, these results show that $\gamma\delta$ T cells are part of a network of immune cells in the tumour microenvironment involved in tumour progression and metastasis. Indeed, various clinical studies have indicated a role of neutrophils, $\gamma\delta$ T cells, IL-17 and macrophages in metastasis [61-63]. With these data, Coffelt and colleagues have defined a metastatic cascade in which IL-1 β stimulates IL-17-producing $\gamma\delta$ T cells to induce neutrophil polarisation and expansion, which suppresses CD8⁺ T cells and therefore promotes tumour progression and metastasis.

1.4.2 BRCA1-deficient cancer model

In this study, the role of BRCA1 in mammary tumourigenesis was investigated. To this end, a conditional mouse model of triple negative breast cancer was used. Similar to KEP mice, the tumour model is based on the knockout of epithelial-specific *P53* combined with epithelial-specific loss of BRCA1. The generation of this mouse model has been described previously [64]. The *K14-Cre;Brca1^{F/F};Trp53^{F/F}* (KB1P) and *K14-Cre;Trp53^{F/F}* (KP) mice in our cohort were found to reach clinical endpoint as a result of one or more mammary tumours after 36 or 45 weeks, respectively (figure 1A). The mammary tumours that develop in KB1P mice are predominately (90%) pure epithelial tumours (carcinomas). Other mammary tumours are biphasic. In KP mice, approximately 40% of the tumours are epithelial tumours, half of the tumours classify as carcinosarcomas (50%) and the remainder are adenomyoepitheliomas (figure 1B, C). In addition, these mice also develop skin carcinomas, showing that *P53* and *BRCA1* collaborate in both skin and mammary tumourigenesis.

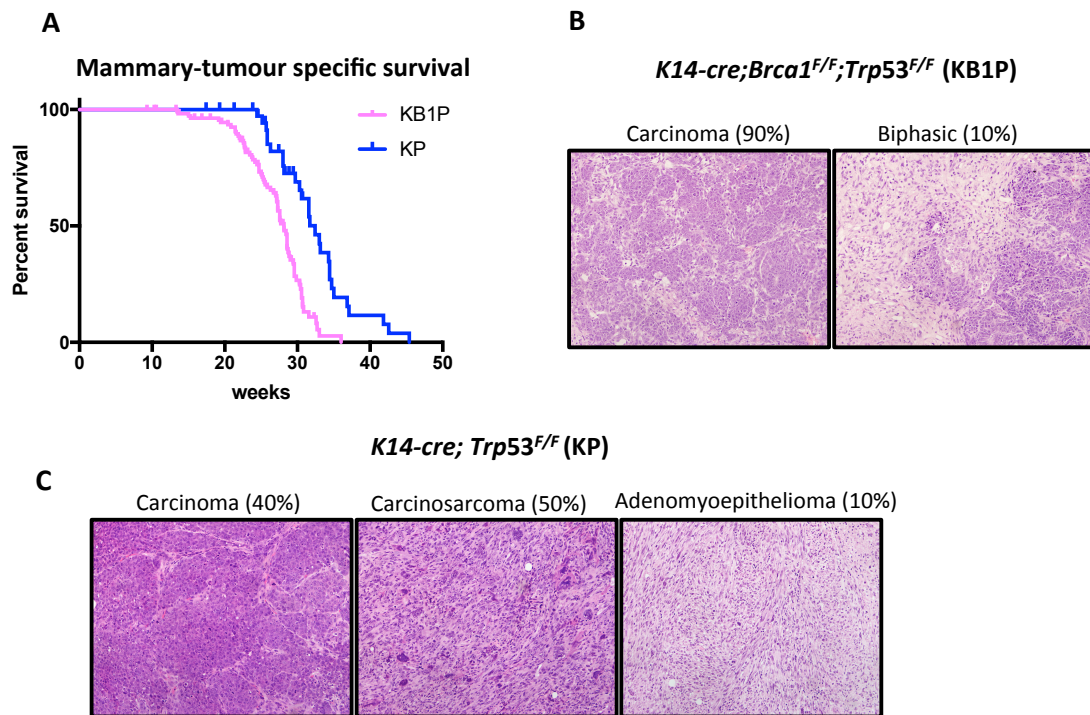


Figure 1. BRCA1-deficient mammary tumour model. (A) Mammary-tumour specific survival in KB1P and KP mice. (B-C) Histopathology of mammary tumours in (B) KB1P and (C) KP mice. Mice were sacrificed at clinical endpoint and mammary tumour tissue sections were stained with Mayer's haematoxylin and eosin. Images are representative of at least 5 individual tumours from each cohort.

1.4.3. RON-MSP axis in breast cancer metastasis

Previous results showed that the $\gamma\delta$ T cell - IL-17 - neutrophil cascade promotes metastasis in breast cancer. In turn, this cascade is induced by IL-1 β in the tumour microenvironment, which is predominantly secreted by macrophages. However, the mechanism remains elusive. Considering the fact that macrophages are key players in tumourigenesis, any receptor that is expressed on macrophages could contribute to their pro-tumourigenic potential. Recently, macrophage stimulating 1-receptor (MSTR1), also referred to as Recepteur d'Origine nantais (RON), has gained more attention. RON is a receptor tyrosine kinase (RTK) and predominantly expressed on macrophages and epithelial cells. RTKs are transmembrane proteins consisting of an extracellular ligand-binding domain and an intracellular tyrosine kinase domain. The transmembrane domain holds the receptor at the cell surface and separates the extracellular ligand-binding domain and the intracellular tyrosine kinase domain [65]. RON is part of the MET family of RTKs and shares high homology (60%) with the oncogene *c-MET* in its kinase domain [66]. Similar to *MET*, RON is translated into a precursor protein and undergoes further proteolytic cleavage, which results in its mature, form, consisting of an α and β subunit linked by disulphide bonds. In both normal and cancerous tissues, two *RON* transcripts are commonly observed as a result of two promoter initiation sites. Moreover, these two promoter start sites are highly conserved in different species, including human and mouse. The full-length *RON* transcript stems from the classical *RON* promoter upstream of the initiation site. The short form *RON* (SF-*RON*) transcript makes use of an alternative promoter, resulting in a truncated form, which lacks the extracellular ligand-binding domain of *RON* and is constitutively active [67]. Additionally, several isoforms of the *RON*

protein have been reported. These isoforms can be constitutively active, oncogenic or biologically inactive [68].

The only known ligand for RON is macrophage-stimulating protein (MSP), which is encoded by the *Mst1* gene. MSP is structurally similar to hepatocyte growth factor, the ligand of MET. Binding of MSP to RON activates several downstream signalling pathways, including PI3K/Akt, MAPK/ERK, β -catenin and JAK/STAT, which results in proliferation, migration, invasion and survival of cancer cells [69]. The RON receptor is overexpressed in many human cancers, including breast, colon, lung, thyroid, skin, bladder and pancreas cancers [70, 71]. In breast cancer, RON is overexpressed in approximately 50%-100% of the tumours and is associated with an aggressive phenotype and poor prognosis [70, 72, 73]. In addition to overexpression of RON, oncogenic variants of RON and constitutive activation of downstream signalling pathways have been found in various tumours and cancer cell lines (reviewed in [67, 68]).

Several studies show that RON and SF-RON are involved in breast cancer metastasis. For example, Liu *et al.* used MCF7 cells *in vitro* and also orthotopically injected MCF7, MFC7-RON and MCF7-sfRON cells in NOD/SCID mice. They showed that MCF7-sfRON cells increased tumour growth and metastasis through activation of PI3K, whereas MCF7-RON cells did not have this effect on tumourigenesis [74]. Eyob *et al* used *MMTV-PyMT* mice (FVB), from which they isolated the tumours. These *MMTV-PyMT* tumours were transduced to overexpress MSP (described in [73]) and the *PyMT*-MSP tumour cells were then transplanted into the cleared mammary fat pad of wild type and RON-deficient syngeneic mice. They demonstrated that loss of RON signalling blocks metastasis to the lung, but had no significant effect on primary tumour growth and progression [75].

Importantly, loss of RON function promoted a more effective anti-tumour response by CD8⁺ T cells, indicating that the RON/MSP axis promotes tumour metastasis by abrogating anti-tumour responses. Indeed, they crossed RON-deficient mice with NOD/SCID mice and showed that these RON deficient, immune-incompetent mice showed normal metastasis, whereas immune-competent RON deficient mice were nearly free of metastases [75]. Furthermore, a decrease in metastatic tumour growth in wild type mice was achieved using the RON inhibitor BMS-777607, not only when the mice were pre-treated with the inhibitor, but also after metastases had been established, which resembles the clinical setting more closely. However, when CD8⁺ T cells were depleted with anti-CD8⁺ antibodies in RON-deficient mice, metastasis could not be inhibited, suggesting that the cytotoxic T cell response is necessary for the anti-metastatic effect of BMS-777607 [75]. Similarly, Gurusamy *et al.* orthotopically transplanted prostate cancer cells (TRAMP-C2Re3) into the prostates of wild-type and RON-deficient mice (C57BL/6) and demonstrated that RON is involved tumour growth [76]. Moreover, they crossed LysMrce⁺ mice with homozygous Ron-floxed mice to generate Ron-floxed LysMrce⁺, which show deletion of RON in myeloid cells. Using the Ron-floxed LysMcre⁺ mice, they showed that loss of RON was sufficient to inhibit prostate cancer growth. Furthermore, they found that depletion of CD8⁺ T cells, but not CD4⁺ T cells, restores tumour growth [76].

Thus, inhibition of RON signalling in macrophages is an interesting target to abrogate tumorigenesis. Indeed, previous microarray results showed that BRCA1-proficient (KP) and BRCA1-deficient (KB1P) mammary tumours have strikingly similar expression profiles of immune-related genes [77]. *Mst1*, the gene that encodes for MSP was the only immune-related gene that was overexpressed in BRCA1-deficient

mammary tumours, suggesting an important role of the RON-MSP axis in BRCA1-deficient breast cancer.

1.4.4. Anti-tumour IFN γ -producing $\gamma\delta$ T cells

As mentioned, neutrophil abundance is an independent prognostic factor for metastasis and subsequent worsened metastasis-specific survival in breast cancer patients [78]. Accumulation of $\gamma\delta$ cells in primary tumours correlates with increased metastasis and decreased overall survival [63]. Previous data have provided a mechanistic explanation for these clinical observations [58]. The pro-tumourigenic IL-17-producing $\gamma\delta$ cells involved in metastasis are phenotypically and functionally distinct from IFN γ -producing $\gamma\delta$ T cells. IFN γ -producing $\gamma\delta$ T cells are proposed to have anti-tumourigenic properties. In skin, prostate and melanoma models, they were found to control cancer progression [79-81]. However, their role in breast cancer metastasis is unknown.

The purpose of this study was twofold. We used *K14-Cre;Brca1^{F/F};Trp53^{F/F}* (KB1P) and *K14-Cre;Trp53^{F/F}* (KP) mice to elucidate the possible role of the RON-MSP axis in BRCA1-deficient breast cancer metastasis. In addition, our interest was to study the function of IFN γ -producing $\gamma\delta$ T cells in triple negative breast cancer with the goal to improve their anti-tumourigenic potential. We hypothesised that the anti-metastatic properties of these IFN γ -producing $\gamma\delta$ T cells are suppressed by the immunosuppressive phenotype of neutrophils. In addition, we hypothesise that RON-MSP signalling stimulates IL-1 β secretion by macrophages from the mammary tumour microenvironment in order to initiate the $\gamma\delta$ T cell - IL-17 - neutrophil metastatic cascade. Ultimately, our long-term goal is to develop new combinatorial

approaches targeting both cancer cells and immune cells to abrogate breast cancer metastasis.

Chapter II. Materials and methods

2.1 Mice and animal experiments

The generation and characterisation of *K14-Cre;Brca1^{F/F};Trp53^{F/F}* (KB1P) and *K14-Cre;Trp53^{F/F}* (KP) mice, two models of breast cancer has been described [64]. KB1P and KP mice were backcrossed onto the FVB/N background (>8 generations). Genotyping was outsourced to Transnetyx, Inc. Mice were monitored two times a week for mammary tumour formation by palpation and caliper measurements from 3 months of age. Clinical endpoint was defined as any tumour with a diameter of 15 mm. Mice were sacrificed at endpoint and tissues were collected in ice-cold PBS, 10% formalin or on ice for flow cytometry, immunohistochemistry or Western blot experiments, respectively. Blood samples were collected in heparin containing tubes or processed for serum. Control mice were age-matched.

For pilot immune cell depletion experiments, wild-type FVB/N mice (Charles River) were treated (IP) with anti-V γ 1 (clone 2.11; BioXCell) once a day for three consecutive days with 400 μ g, followed by two doses of 200 μ g. Mice were sacrificed on the fourth day. Lymph nodes, lungs and blood were collected for analysis. To test drug tolerance to RON/c-MET dual inhibitor BMS777607, wild-type FVB/N mice were administered 50 mg/kg BMS777607 (dissolved in DMSO and diluted in 70% PEG-300) or vehicle control (11% DMSO diluted in 70% PEG-300) by oral gavage once a day for 5 consecutive days per week, for a total of 12 days. Mice were sacrificed on day 13. General animal health and weight (less than 10% weight loss at any point during treatment) were used as a measurement of drug tolerance. Control mice received equal amounts of isotype control antibodies or vehicle and mice were randomised before the start of treatment.

Animals were housed in individually ventilated open cages on a 12/12-h light/dark cycle and fed and watered *ad libitum*. The mouse experiments were performed under UK Home Office license number 70/8645. Experiments were carried out in line with the Animals (Scientific Procedures) Act 1986 and the EU Directive 2010 and were sanctioned by the local ethical review process (University of Glasgow).

2.2 Generation of primary mouse breast cancer cell lines and cell culture

Primary breast cancer cell lines were established from mammary tumours grown to endpoint in KB1P and KP mice. Tumours were collected on ice-cold PBS and digested with 2 mg/mL collagenase A (Roche) and 100 µg/mL DNaseI in serum-free Dulbecco's modified Eagle's medium (DMEM) (Gibco) using the gentleMACS[®] Octo with heaters dissociation system (Miltenyi) according to manufacturer's directions. Subsequently, cells were dispersed through a 70 µM cell strainer. Single cell suspensions were plated and propagated under hypoxic conditions (37°C, 5% CO₂, 3% O₂) for 4 weeks. Multiple rounds of differential trypsinisation were used to select for epithelial cells. The immortalised epithelial cells were expanded and used for further experiments.

Individual cell lines (2 KP and 2 KB1P) were derived from independent donor tumours and designated KP-1, KP-2, KB1P-1 and KB1P-2. Cells were grown and maintained in DMEM, supplemented with 10% foetal bovine serum (FBS) (Gibco), 100 IU/mL penicillin (Gibco) and 100 µg/mL streptomycin (Gibco) and 2 mM L-glutamine (Gibco) under hypoxic conditions (37°C, 5% CO₂, 3% O₂). All cell lines were never split more than ten times upon receipt and tested in-house for Mycoplasma.

RON/c-MET dual inhibitor BMS-777607 (Chemietek, #CT-BMS777) was dissolved in dimethyl sulfoxide (DMSO) and recombinant MSP (6244-MS-025; R&D

Systems) was dissolved in PBS/0.1% BSA. Compounds were added to the culture medium at the indicated concentrations. Equal volumes of DMSO and/or PBS/0.1% BSA were added to the medium, as vehicle controls.

2.3 Western blotting

Mammary tumours were collected on ice and lysed in RIPA buffer, supplemented with HALT™ protease and phosphatase inhibitor cocktail (Thermo Scientific), using the Precellys hard tissue homogenising lysing kit (Bertin Instruments) in a Precellys tissue homogeniser (Bertin Instruments). Harvested lysates were clarified by centrifugation at 13,000 g for 20 min at 4°C and protein concentration of the supernatants was determined using the Micro BCA protein kit (Thermo Scientific). Equal amounts of proteins were separated (120V, 2 hrs) on 4-12% Bolt Bis-Tris gels using the Bolt electrophoresis systems (Invitrogen) with Bolt MOPS SDS running buffer (Invitrogen). Separated proteins were transferred onto nitrocellulose membranes using the iBlot2® system (Invitrogen) according to manufacturer's instructions. Membranes were blocked in Odyssey PBS blocking buffer (LI-COR) and immunostained with the protein of interest. Proteins were detected with appropriate secondary antibodies labelled for detection in the 700 or 800 nm channel on an Odyssey Infrared imaging System (LI-COR), respectively.

The antibodies used were as follows: Anti-MSP (#AF6244, 1:1000; R&D systems), β -actin (#A5316, 1:5000; Sigma), Goat-anti-rabbit-IRDye 680RD (#925-68071, 1:10000, LICOR), Goat-anti-mouse-IRDye 800CW (#925-32210, 1:10000, LICOR) and Donkey-anti-sheep-Alexa Fluor 680 (#A21102, 1:10000, Invitrogen). Two RON antibodies were tested and not used in final experiments due to inconsistent or lack of staining:

Anti-RON (#LS-C164490, LifeSpan), Anti-RON (#ab52927, Abcam). Antibodies were diluted in Odyssey PBS blocking buffer/0.1% Tween-20 (Sigma).

2.4 Immunohistochemistry

Mammary tumours were fixed in 10% buffered formalin and embedded in paraffin wax. Tissue sections were stained with Mayer's haematoxylin and eosin (H&E) according to routine procedures. For antibody staining, tissue sections were deparaffinised and rehydrated by immersion in Xylene, ethanol and water and incubated with citrate buffer (DAKO). Slides were blocked with goat serum (Vector labs)/2.5% BSA in TBS/0.05% Tween-20 for 30 min at RT. Primary antibodies were diluted in antibody diluent (DAKO) and incubated ON at 4°C. Endogenous peroxidase was quenched using peroxidase block (DAKO) and slides were stained with the appropriate secondary HRP-conjugated antibody. Staining was visualised by DAB staining, and slides were counterstained with haematoxylin and mounted in DPX according to routine procedures. The antibodies used were as follows: anti-MSP (#MAB6244, 1:20, R&D systems), anti-rabbit-HRP (DAKO), anti-rat-HRP (Vector labs). Images were captured on an Axio Imager A2 Bio upright microscope (Zeiss) using ZENPRO 2012 software (Zeiss).

2.5 ELISA

Blood from mice was collected at endpoint and processed to obtain serum. Serum was diluted 1:400 and MSP concentration was determined using the Quantikine ELISA mouse MSP/MST1 kit according to manufacturer's directions. Absorbance was measured at 450 nm and 540 nm. Readings at 540 nm were subtracted from 450 nm readings.

2.6 Cell viability assay - crystal violet

10,000 KP or KB1P cells were plated in 24-well plates (Corning) in growth medium.

Cells were allowed to attach overnight and washed with PBS and grown under the indicated conditions in DMEM, supplemented with 0.2% FBS, 100 IU/mL penicillin, and 100 µg/mL streptomycin. After 72 hours, cells were washed in PBS and adherent cells were fixed in 4% formaldehyde solution (Sigma) and stained with 0.1% crystal violet solution (Sigma). Stained cells were imaged using a desktop scanner (Epson). Crystal violet dye was dissolved in 10% acetic acid (Fisher chemical) and quantified at 590 nm in a multimode microplate reader (Tecan).

2.7 Flow cytometry - surface and intracellular staining

Tissues were collected in ice-cold PBS. Lungs and tumours were digested in serum-free DMEM supplemented with 1 mg/ml collagenase D (Roche) and 25 µg/mL DNase I (Roche), or 2 mg/mL collagenase A (Roche) and 100 µg/mL DNaseI, respectively. Tissues were processed using the gentleMACS® with heaters dissociation system (Miltenyi) according to manufacturer's directions. Cells were filtered through a 70 µM cell strainer and 10% cold FCS was added to neutralise the enzyme reaction. Lymph nodes and liver were mashed through a 70 µM cell strainer in PBS/0.5% BSA. All cell suspensions were treated with red blood cell (RBC) lysis buffer (eBioscience) and then re-suspended in PBS/0.5% BSA.

For lungs and tumour tissues, 4×10^6 cells were plated and 2×10^6 cells were used for lymph nodes and liver tissues. To increase labelling specificity, Fc receptors were blocked before surface staining using TruStain FcX™ (anti-mouse CD16/32) antibody (Biolegend) according to manufacturer's instructions. Cells were stained for surface proteins with directly conjugated antibodies in BD Brilliant™ stain buffer (BD

biosciences) for 30 min at 4°C, in the dark. After surface staining, fixable viability dyes Zombie NIR (APC-eFluor780) or Zombie green (FITC) (Biolegend) were added for 20 min at 4°C in the dark to exclude dead cells. For intracellular staining, cells were first stimulated for 3 hours at 37°C with 2 ul/mL cell stimulation cocktail plus protein transport inhibitors (PMA, Ionomycin, Brefaldin A and Monensin) (eBioscience) in IMDM containing 8% FBS, 100 IU/mL penicillin, 100 ug/mL streptomycin, supplemented with 0.5% β -mercaptoethanol. Surface proteins were stained after cell stimulation. Subsequently, cells were fixed and permeabilised using the intracellular fixation and permeabilisation kit (eBioscience), followed by intracellular staining in permeabilisation buffer for 30 min at 4°C, in the dark. Cells were analysed using a BD LSRFortessa™ flow cytometer using Diva software (BD biosciences). Results were analysed using FlowJo Software, version 9.9.6. (Treestar).

The antibodies were purchased from eBioscience (CD45, CD11c, MHCII, CD80, Anti-rabbit, PCDA-1/CD317, EpCAM/CD326, TER-119, CD3, CD19-FITC, CD19-APC-eFluor780, $\gamma\delta$ TCR, CD11b-APC-eFluor780, V γ 4, IFN γ -PE-Cy7, IFN γ -eFluor450, IL-17A-PE and IL-17A-APC), Biolegend (CD11b, F480, Ly6C, CD103, Rabbit isotype control, CD27, CD3, CD4-BV605, CD44, NKp46, CD69, V γ 1, Granzyme B) or BD (Ly6G, CD4-BUV563, CD8-BUV395, CD8-BUV805), apart from the RON antibody, which was purchased from Abcam (#ab52927). All antibodies were titrated and three different multicolour flow cytometry panels were designed and optimised. The RON antibody and rabbit isotype control were excluded from the optimised panel designs, as antibody showed inconsistent results and was rendered incompatible with flow cytometry applications. The optimised panels were composed of the following antibodies:

Myeloid panel - CD45-eVolve605 (1:100, clone 30-F11), CD11b-BV785 (1:400, clone M1/70), F480-BV650 (1:50, clone BM8), CD11c-PE-Cy5 (1:200, clone N418), Ly6G-BUV395 (1:50, clone 1A8), Ly6C-PE/Dazzle594 (1:200, clone HK1.4), MHCII-PerCP-eFluor710(1:100, cloneM5/114.15.2),CD103-BV421(1:200, clone 2E7), CD80-APC (1:50 clone 16-10A1), PDCA-1/CD317-PE-Cy7 (1:400, clone eBio927), EpCAM/CD326-APC-eFluor78- (1:50, clone G8.8), TER-119-FITC (1:100, clone TER-119), CD3-FITC (1:100, clone 145-2C11), CD19-FITC (1:800, clone eBio1D3), fixable viability dye-FITC (Zombie Green).

T cell activation panel - CD27-PE/Dazzle594 (1:400,clone 1D3), CD3-BV650 (1:100, clone 17A2), $\gamma\delta$ TCR-FITC (1:200, clone GL3), CD4-BV605 (1:100, clone GK1.5),CD8-BUV395 (1:100, clone 53-6.7), CD44-PerCP-Cy5.5 (1:100, clone IM7), NKp46-BV421 (1:100, clone 29A1.4), CD69-BV510 (1:50, clone H1.2F3), CD11b-BV785 (1:800, clone M1/70). CD19-APC-eFluor780 (1:400, clone 1D3), EpCAM/CD326 (1:100 clone G8.8) IFN γ -PE-Cy7 (1:200, clone XMG1.2), IL-17A-PE (1:100, clone eBio17B7), Granzyme B-AlexaFluor-647 (1:50, clone GB11), fixable viability dye-APC-eFluor 780 (Zombie NIR).

V γ 1/V γ 4 TCR usage panel - CD27-PE/Dazzle594 (1:400,clone 1D3), CD3-BV650 (1:100, clone 17A2), $\gamma\delta$ TCR-FITC (1:200, clone GL3), CD4-BUV563 (1:100, clone GK1.5), CD8-BUV805 (1:50, clone 53-6.7), V γ 1-PE (1:200, clone 2.11), V γ 4-PE-Cy7 (1:100, clone UC3-10A6), IFN γ -eFluor450 (1:200, clone XMG1.2), IL-17A-APC (1:100, clone eBio17B7), CD11b-APC-eFluor780 (1:800, clone M1/70), CD19-APC-eFluor780 (1:400, clone 1D3), EpCAM/CD326 (1:100, clone G8.8), IFN γ -eFluor450 (1:200, clone

XMG1.2), IL-17A-APC (1:100, clone eBio17B7), Fixable Viability dye-APC-eFluor 780 (Zombie NIR).

2.8 Real-time cytotoxicity assay

10,000 KP or KB1P cells were plated in 24-well plates (Corning) in growth medium.

Cells were allowed to attach overnight and washed with PBS and grown under the

indicated conditions in DMEM, supplemented with 0.2% FBS, 100 IU/mL penicillin,

100 ug/mL streptomycin and 30 nM Sytox green (Invitrogen). Every well was imaged

(phase-contrast, green fluorescence) for 48 hours, with a 2 hr interval using an

IncuCyte ZOOM life cell imaging system (Essen BioScience). The change in green

fluorescence was used to determine the cytotoxicity curves as a measurement of cell death.

2.9 Invasion assay

96-well Imagelock® plates (Essen BioScience) were coated with growth factor

reduced matrigel (Corning) at 100 µg/ml in growth medium overnight at 37°C.

Matrigel was removed and 30,000 KB1P cells were plated in growth medium and

incubated for 4 hours at 37°C to form a monolayer. Cells were wounded with a

WoundMaker™ 96 (Essen BioScience). Wounds were cleared of debris by washing

with DMEM, supplemented with 0.2% FBS, 100 IU/mL penicillin, 100 ug/mL

streptomycin. 25% matrigel in DMEM, containing the indicated drug compounds

was added to each invasion well. Matrigel was allowed to set at 37°C for 1 hr and

medium containing the same drug compounds was added on top of the matrigel.

Cells were imaged every hour using an IncuCyte S3 life cell imaging system (Essen

BioScience). The change in relative wound density (RWD) over time measured by the

IncuCyte software was used as a measurement for invasion.

2.10 Statistical analysis

The nonparametric Mann-Whitney *U*-test was used when comparing two groups.

The Kruskal-Wallis *H*-test was used when comparing three or more groups. Analyses were performed using Graphpad PRISM (version 7; GraphPad). P values ≤ 0.05 were considered significant.

Chapter III. Results

3.1 BRCA1-deficient mice show neutrophilia and IL-17-producing $\gamma\delta$ T cells are increased in BRCA1-deficient mice

Previous data using a mouse model of lobular breast cancer have indicated that IL-17-producing $\gamma\delta$ T cells promote metastasis by stimulating the immunosuppressive phenotype of neutrophils. We asked the question whether this $\gamma\delta$ T cell-IL-17-neutrophils axis also has importance in BRCA1-deficient (i.e. triple negative) breast cancer. To this end, we assessed neutrophil expansion in the blood and the presence of IL-17-producing $\gamma\delta$ T cells in lymph nodes and lungs of wild-type mice and tumour-bearing KB1P mice. Blood, lymph nodes and lungs were taken from KB1P mice at clinical endpoint. Wild type tumour free littermates were used as control mice. Lung and lymph nodes were processed, and both surface staining and intracellular staining was performed using the T cell activation flow cytometry panel. Staining of cytokines IFN γ and IL-17A on the $\gamma\delta$ T cells (CD3⁺ CD4⁻ CD8⁻ $\gamma\delta$ TCR⁺) shows two distinct $\gamma\delta$ T cell subpopulations (figure 2A). More specifically, the results expectedly show that IFN γ and IL-17A expression on $\gamma\delta$ T cells is mutually exclusive, supporting the fact that IFN γ and IL-17A-producing $\gamma\delta$ T cells are phenotypically different from one another. The number of IL-17-producing $\gamma\delta$ T cells in the total $\gamma\delta$ T cell population was increased in tumour-bearing KB1P mice. In the lymph nodes of KB1P and wild-type mice, 5% and 8% of the $\gamma\delta$ T cell population was composed of IL-17-producing $\gamma\delta$ T cells, respectively (figure 2B). This increase was more pronounced in the lung of KB1P mice, in which nearly 50% of the $\gamma\delta$ T cells were IL-17-producing $\gamma\delta$ T cells compared to 25% in wild-type mice (figure 2B). Blood analysis showed that neutrophils made up 15% of the immune cell composition in wild type tumour free

mice. In contrast, tumour-bearing KB1P mice showed neutrophilia, with neutrophils making up 40% of the immune cell composition in the blood (figure 2C). These data indicate that the $\gamma\delta$ T cell-IL-17-neutrophils axis is also important in metastasis formation in other mammary tumour models, including BRCA1-deficient breast cancer.

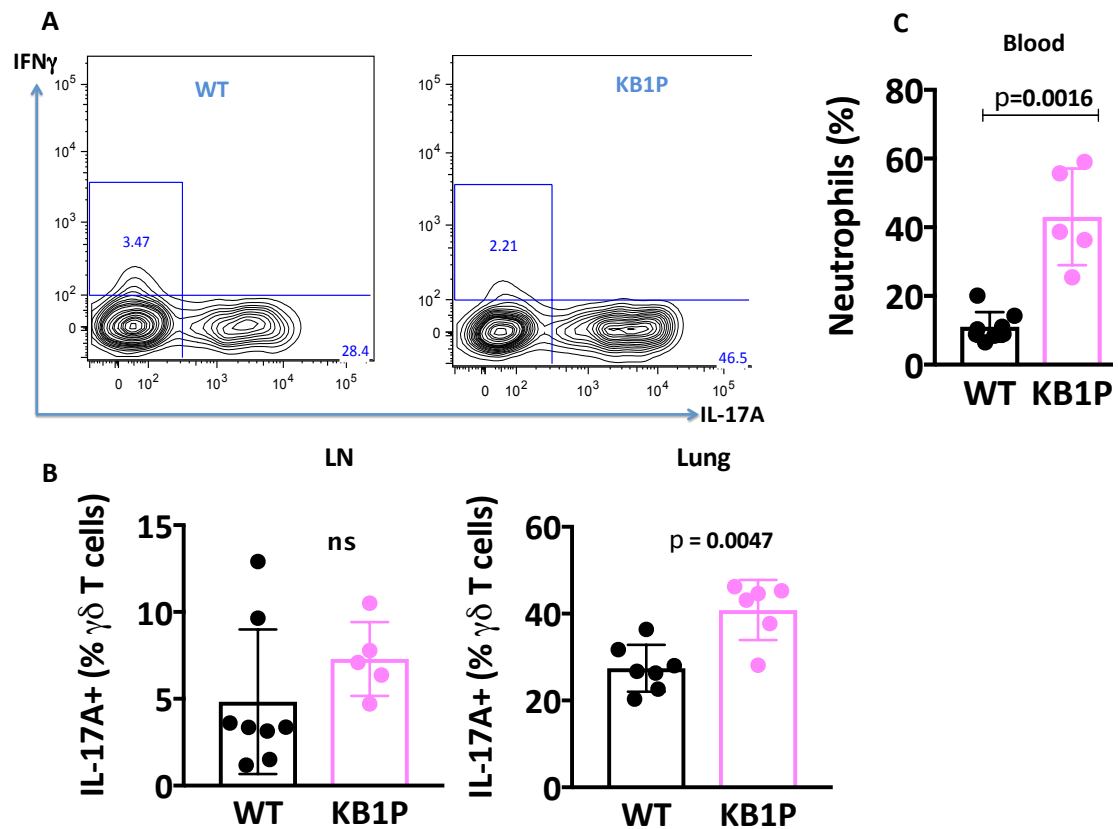


Figure 2. $\gamma\delta$ T cells and neutrophils in wild type and BRCA1-deficient mice. (A) Representative images of IFN γ -IL-17A flow gate from $\gamma\delta$ T cell parent gate. (B) IL-17-producing $\gamma\delta$ T cells in wild type and KB1P mice (LN: n = 8 WT, n = 5 KB1P; Lung: n = 7 WT, n = 6; Mann-Whitney test). (C) Neutrophils in blood of wild type (n=6) and KB1P mice (n = 5). Lungs, lymph nodes and blood were collected from mice at clinical endpoint. Lungs were digested with collagenase D and red blood cells were lysed. Remaining cells were collected and incubated with antibodies using a 10-colour T cell flow cytometry panel. B-lymphocytes (CD19) and epithelial cells (EpCAM) were gated out by means of a dump channel (APC-eFluor780). The percentages shown represent the frequency of cells relative to the parent gate. Immune cell populations are shown as proportion of the total amount of $\gamma\delta$ T cells. Blood was analysed on an Idexx ProCyte Dx Hematology Analyzer. All data are mean (SD).

3.2 MSP expression, but not RON expression is increased in mammary tumours of BRCA1-deficient mice

The observed neutrophilia and increase of IL-17-producing $\gamma\delta$ T cells in KB1P mammary tumours suggests an importance of the IL-17-neutrophils axis in BRCA1-deficient breast cancer. However, the process by which cancer cells drive this metastatic cascade remains elusive. Considering the fact that previous microarray data show an increase in *Mst1* in KB1P mammary tumours, but not in KP mammary tumours [77], we wondered whether MSP was overexpressed in the mammary tumours of KB1P mice. QPCR data (QPCR performed by other members of the lab) show an increase in *Mst1* expression in the mammary tumours of KB1P mice, compared to KP mice (figure 3A). The expression of *Mst1r*, the gene encoding for the receptor RON, was also assessed. Interestingly, RNA expression of *Mst1r* was similar in the mammary tumours of KB1P and KP mice (figure 3B). In order to determine whether the increase in RNA expression had an effect on translation, MSP protein expression was assessed. To this end, mammary tumours of KB1P and KP mice at clinical endpoint were analysed by Western blot. Lung tissue from wild type tumour-free mice was used as a negative control. Western blot analysis shows that MSP protein expression reflects mRNA levels and is increased in KB1P-derived mammary tumours compared to KP-derived mammary tumours (figure 3C). These data suggest that activation of RON-MSP axis through overexpression of MSP could play a role in metastasis in BRCA1-deficient mice.

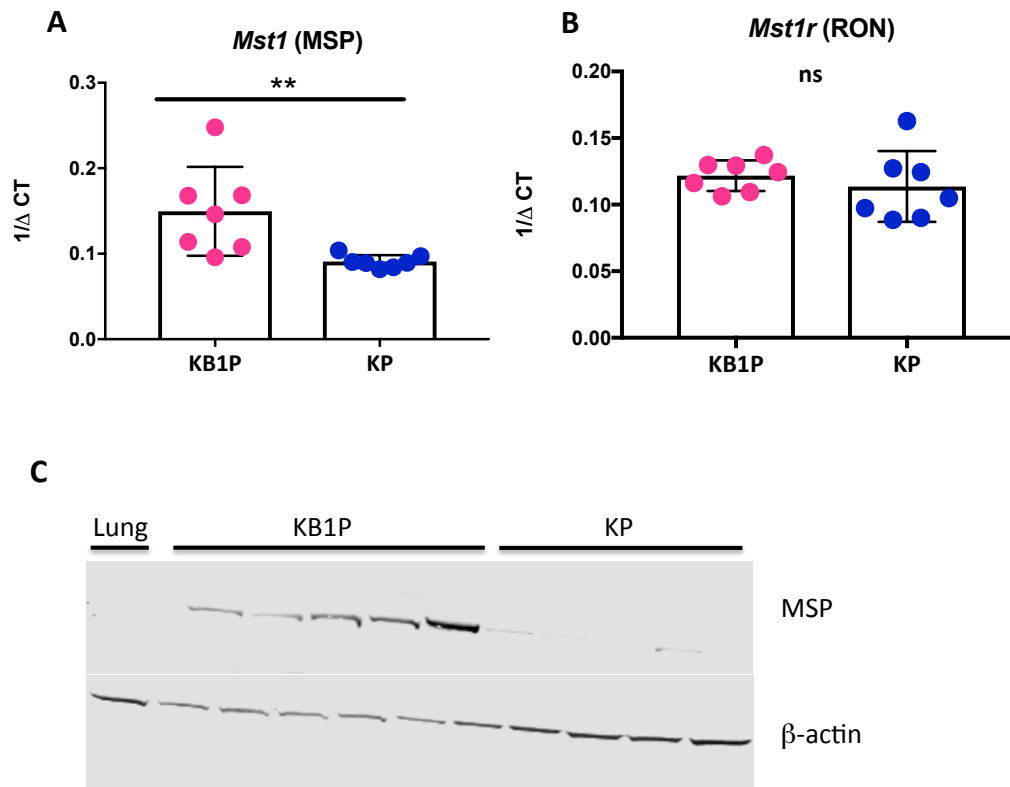


Figure 3. RON and MSP expression in BRCA1-deficient (KB1P) and BRCA1-proficient (KP) mammary tumours. (A) Real-time PCR of *Mst1* and *Mst1r* mRNA expression (n = 5 KB1P, n = 5 KP; Mann-Whitney test). (B) Western blot analysis of MSP expression in KB1P and KP tumours (n = 5 KB1P, n = 5 KP, n=1 WT lung). Image is a representation of at least three independent experiments. Mammary tumours were collected from mice at clinical endpoint. Lung tissue for negative control was from age matched wild type mice.

3.3 MSP overexpression does not alter macrophage polarisation in BRCA1-deficient mice and neutrophil infiltration is absent in BRCA1-deficient mammary tumours

Our results showed that MSP is overexpressed in mammary tumours derived from BRCA1-deficient KB1P mice. Since cancer cells manipulate the immune cells in the tumour microenvironment to drive metastasis formation, we hypothesised that the immune cell composition in KB1P and KP mammary tumours would be different as a result of MSP overexpression. Moreover, considering the fact that macrophages in the tumour microenvironment were the main source of IL-1 β facilitating the IL-17-neutrophil axis, we hypothesised that macrophage composition would be different between the mammary tumours. Mammary tumours were collected at clinical endpoint. Tissue was processed and surface staining was performed using the myeloid flow cytometry panel. We observed a significant difference in myeloid (CD11b⁺) cell abundance between BRCA1-proficient KP and BRCA1-deficient KB1P tumours. In KP tumours, 70% of the total immune cell population is composed of myeloid cells, compared to only 20% in KB1P tumours (figure 4A). Interestingly, KP tumours showed an increase in conventional antigen presenting dendritic cells (figure 4B), but not in other dendritic subsets (figure 4D, F). The most striking observation was the difference in neutrophil infiltration in the mammary tumours. Neutrophil infiltration seems absent in KB1P tumours, whereas there is significant infiltration of neutrophils in KP tumours (figure 4E). Unexpectedly, we observed that macrophage abundance was similar between the mammary tumours (figure 4C). We also tried to assess the expression of RON on the macrophages and other immune cell populations. Unfortunately, the results generated with the RON antibody were inconsistent and our isotype control antibody was non-specific so no conclusions could be drawn (data not shown). Although macrophage abundance was unaltered,

MSP could have an effect on macrophage polarisation, without changing macrophage infiltration into the mammary tumours. Previous data have suggested that MHCII expression can be used to define two distinct macrophage populations in tumours. Low MHCII expression is associated with poor antigen-presenting (i.e. pro-tumourigenic) macrophages, whereas good antigen-presenting (i.e. anti-tumourigenic) macrophages have high MHCII expression [82]. Indeed, we could distinguish two macrophage populations based on their MHCII expression. However, we found that macrophage polarisation was similar in the mammary tumours (figure 4G, 4H). In summary, mammary tumours derived from BRCA1-proficient KP mice show an increase in myeloid cells compared to BRCA1-deficient KB1P mice. Unexpectedly, this expansion of the myeloid cell population could not be explained by an increase in macrophage abundance, but is a result of the neutrophil infiltration in these tumours. Furthermore, based on MHCII expression, the macrophages in BRCA1-deficient mammary tumours were not skewed towards a more pro-tumourigenic phenotype.

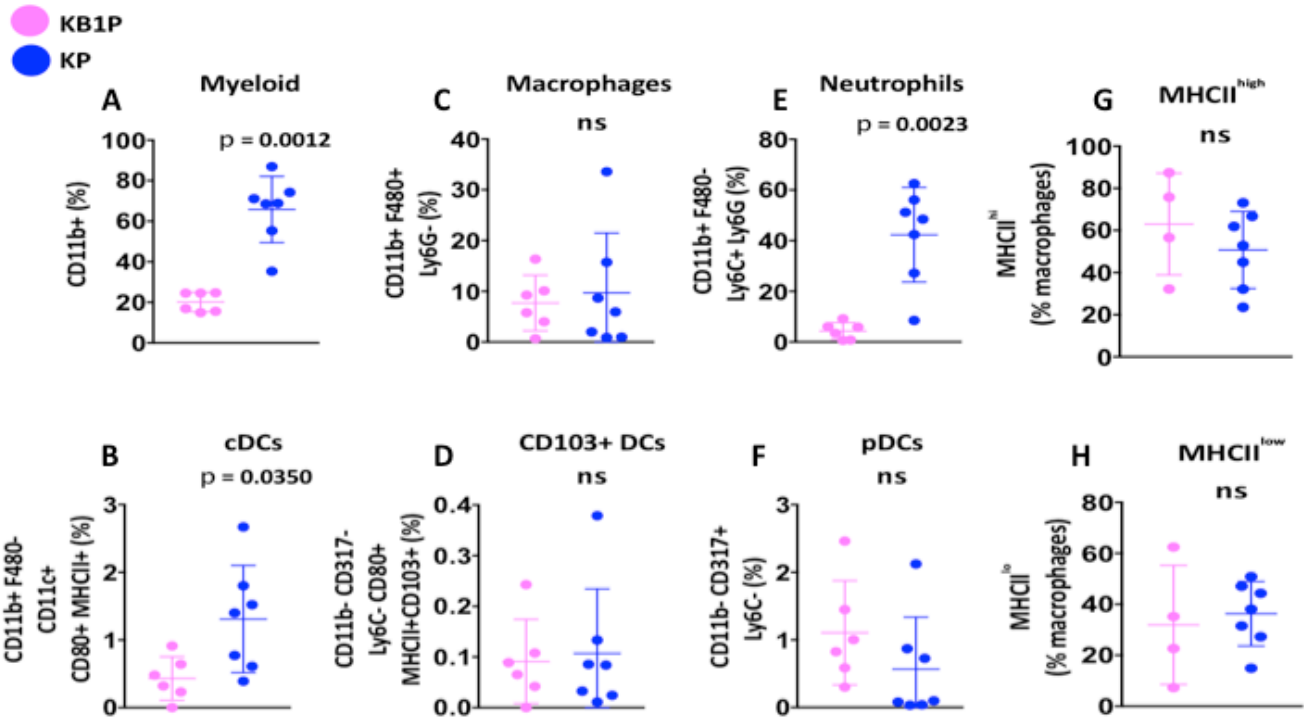


Figure 4. Immune cell composition in mammary tumours of BRCA1-deficient (KB1P) and BRCA1-proficient (KP) mice. Mammary tumours (n = 6 KB1P, n = 7 KP; Mann-Whitney test) were collected from mice at clinical endpoint. Tumours were digested with collagenase A and red blood cells were lysed. Remaining cells were collected and incubated with antibodies using a 12-colour myeloid flow cytometry panel. B-lymphocytes (CD19), T-lymphocytes (CD3) and any remaining blood cells (TER-119) were gated out by means of a dump channel (FITC). The percentages shown represent the frequency of cells relative to the parent gate. Immune cell populations are shown as proportion of the total amount of live cells. All data are mean (SD).

3.4 BRCA1-deficient tumour cells secrete MSP to activate the RON-MSP axis

Surprisingly, the data implicated that MSP overexpression in BRCA1-deficient KB1P mammary tumours does not have a direct effect on the macrophage population in the tumour microenvironment. Therefore, we wondered whether the cancer cells require the RON-MSP axis for their own tumourigenic potential. We hypothesised that the cancer cells secrete MSP to activate the RON-MSP axis. To test this hypothesis, immunohistochemistry was performed to get insight where the MSP protein is located in the tumour microenvironment. Paraffin embedded tumour tissue sections from mice taken at clinical endpoint were stained for MSP. Similar to previous findings, we observed an increased in MSP expression in KB1P mammary tumours (figure 5A) compared to KP mammary tumours (figure 5B). Interestingly, MSP staining was predominantly found around the cancer cells and not in the stromal areas of the mammary tumours (figure 5A, B). Next, with this knowledge and to further elucidate our hypothesis, we assessed the serum levels of MSP in KB1P and KP mice. Serum was collected from wild type tumour-free, KB1P and KP mice at clinical endpoint and the serum levels of MSP were assessed by ELISA. We observed an increase of MSP in the serum of tumour-bearing KB1P mice and KP mice compared to wild type mice. Interestingly, MSP serum levels in KB1P mice were not significantly increased compared to KP mice (figure 5C). These results suggest that the cancer cells possibly secrete MSP in a process of autocrine stimulation.

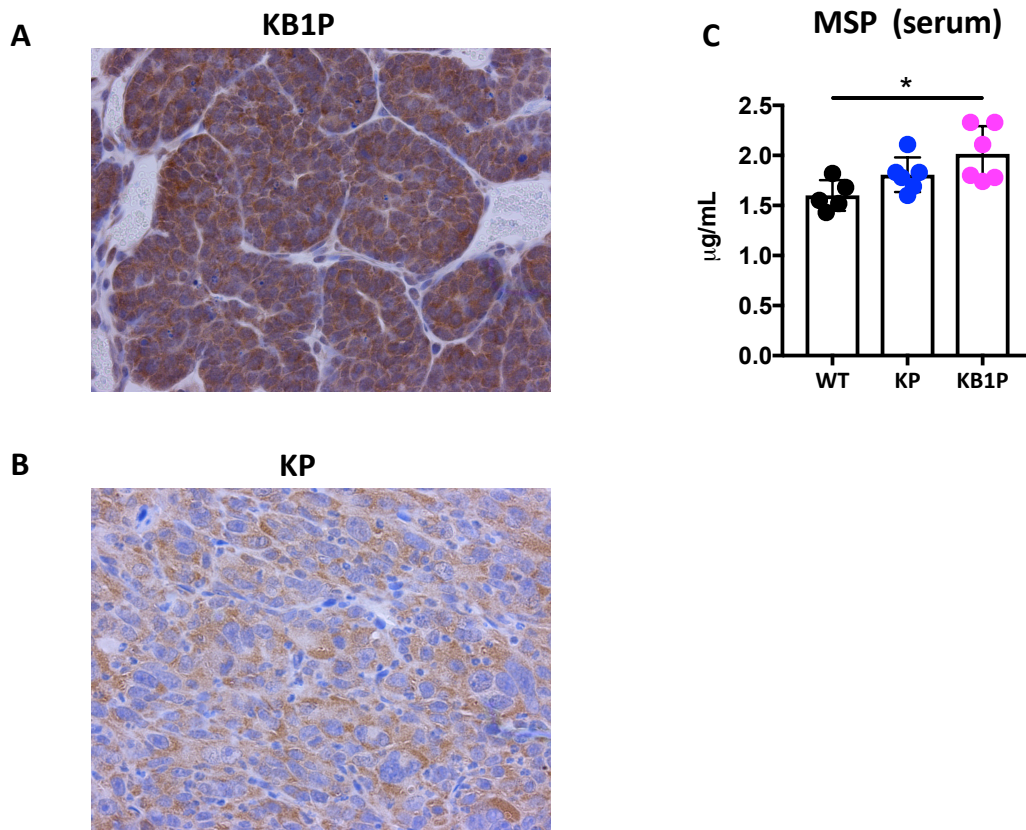


Figure 5. MSP expression and serum levels are increased in KB1P mice. (A) Immunohistochemistry staining of MSP on formalin-fixed paraffin-embedded KB1P and KP tumour sections (heat-antigen retrieval, 40x magnification). (B) MSP serum levels in wild type and tumour bearing KB1P and KP mice (n = 5 wild type, n = 6 KB1P, n = 6 KP; Mann-Whitney *U* test). * $P \leq 0.05$. Mammary tumours and sera were collected from mice at clinical endpoint. Immunohistochemistry images are a representation of at least three independent experiments (n = 8 KB1P, n = 8 KP).

3.5 Inhibition of RON by BMS-777607 does not reduce cell viability in BRCA1-deficient cancer cell lines

To further elucidate the mechanism by which the cancer cells use the RON-MSP axis to facilitate metastasis, we made tumour cell lines from KB1P and KP mammary tumours. Western blot and QPCR analysis performed by other members of the lab confirmed that the tumour cell lines maintained expression of RON after transformation *in vitro* (data not shown). We took a pharmacological approach to target the RON-MSP axis. We hypothesised that if the tumour cell lines require this axis for their tumourigenic potential, the tumour cell lines would be sensitive to treatment with dual MET/RON inhibitor BMS-777607. To this end, we treated 2 KB1P and 2 KP mammary tumour derived cell lines for 72 hours with BMS-777607 or DMSO vehicle in low serum conditions (0.2% FBS). On the fourth day, adherent cells were stained with crystal violet and cell viability was assessed by quantification of crystal violet staining. Treatment with BMS-777607 resulted in reduced cell viability in both KP-1 and KP-2 cell lines (figure 6A). However, treatment with BMS-777607 in the KB1P cell lines had no effect on cell viability (figure 6A). Considering the fact that a reduction in cell viability could be the result of either a reduction in cell proliferation or an increase in cell death, we wondered whether treatment with BMS-777607 induces cell death in KP cell lines. To this end, we performed a real-time cytotoxicity assay using Sytox[®] green. Similar to the experimental setup of the cell viability assay, cells were treated for 72 hours with (increasing concentrations of) BMS-777607 or DMSO vehicle in low serum conditions (0.2% FBS) and green fluorescence was measured at a 1-hour interval. Treatment with BMS-777607 induces cytotoxicity in the KP-2 cell line (figure 6B). Moreover, this cytotoxicity was dose-dependent and became apparent within 24 hours (figure 6C). Since we did not observe reduced cell viability in KB1P tumour cell lines (figure 6A), we hypothesised

that we would not see cytotoxicity in these cells when treated with BMS777607. To test our hypothesis, we treated the KB1P-2 cell line with 2.5 μ M BMS777607. After 24 hours, we observed no increased cytotoxicity in the treated cells versus the control cells, supporting our previous findings that BMS777607 has no effect on cell viability in BRCA1-deficient mammary tumour cell lines (figure 6D).

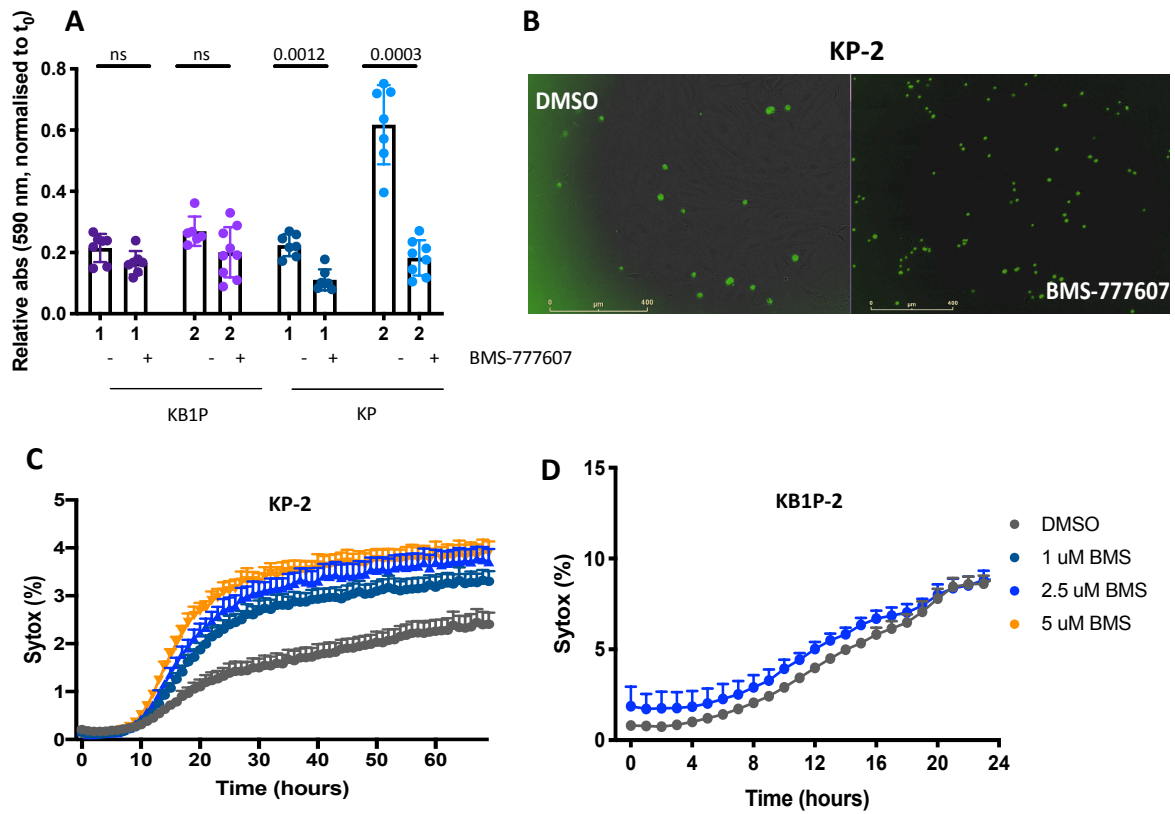


Figure 6. BMS-777607 induces cell death in BRCA1-proficient (KP) tumour cell lines. (A) Cell viability in KB1P (n = 2) and KP (n = 2) cell lines. (B) Representative images of Sytox® green staining in KP-2 cell line in DMSO control and BMS-777607 treated cells. (C) Sytox® green staining in KP-2 cell line treated with BMS-777607. (D) Sytox® green staining in KB1P cell line treated with BMS-777607. Cells were plated and allowed to attach overnight. The next day, cells were treated with DMSO or BMS-777607 at the indicated concentration in low serum conditions (0.2% FBS) for 24 or 72 hours, respectively. Results are representative of at least three independent experiments.

3.6 The RON-MSP axis plays a role in the invasiveness of BRCA1-deficient tumour cells

Our data showed that pharmacological inhibition of the RON-MSP axis had no effect on the cell viability of KB1P cell lines and did not induce cell death. With the knowledge that previous studies have suggested a role of the RON-MSP in breast cancer metastasis and the aggressive phenotype associated with triple negative breast cancer, we wondered whether the RON-MSP axis might contribute to the invasive phenotype of BRCA1-deficient tumour cells. To this end, we performed an invasion/wound-healing assay. We plated KB1P tumour cells and allowed cellular monolayers to form. Next, the cells were wounded and treated with BMS-777607, MSP or the combination at the indicated concentrations in low serum conditions (0.2% FBS). Cells were imaged every hour and the wound density was measured. The change in relative wound density (RWD) over time was used as a measurement for invasion (figure 7C). In order to be able to compare independent experiments, we needed a measurement that does not depend on slight experimental variables (e.g. time). Therefore, we determined $RWD T_{max} \frac{1}{2}$ for each experiment, and used these values for analysis (figure 7A, B). $RWD T_{max} \frac{1}{2}$ is the time at which the RWD of the DMSO control was at 50% RWD. Next, all data was normalised against the DMSO control. Treatment with MSP had no additive effect on the invasiveness of the cell line KB1P-2. We observed a striking reduction (50%) in RWD in KB1P tumour cells treated with BMS777607 and MSP was not able to reverse this effect of BMS-777607 (figure 7C). Initial steps to perform *in vivo* experiments were also taken. To conclude, these data suggest that BRCA1-deficient cancer cells require the RON-MSP axis for their invasive phenotype.

KB1P-2

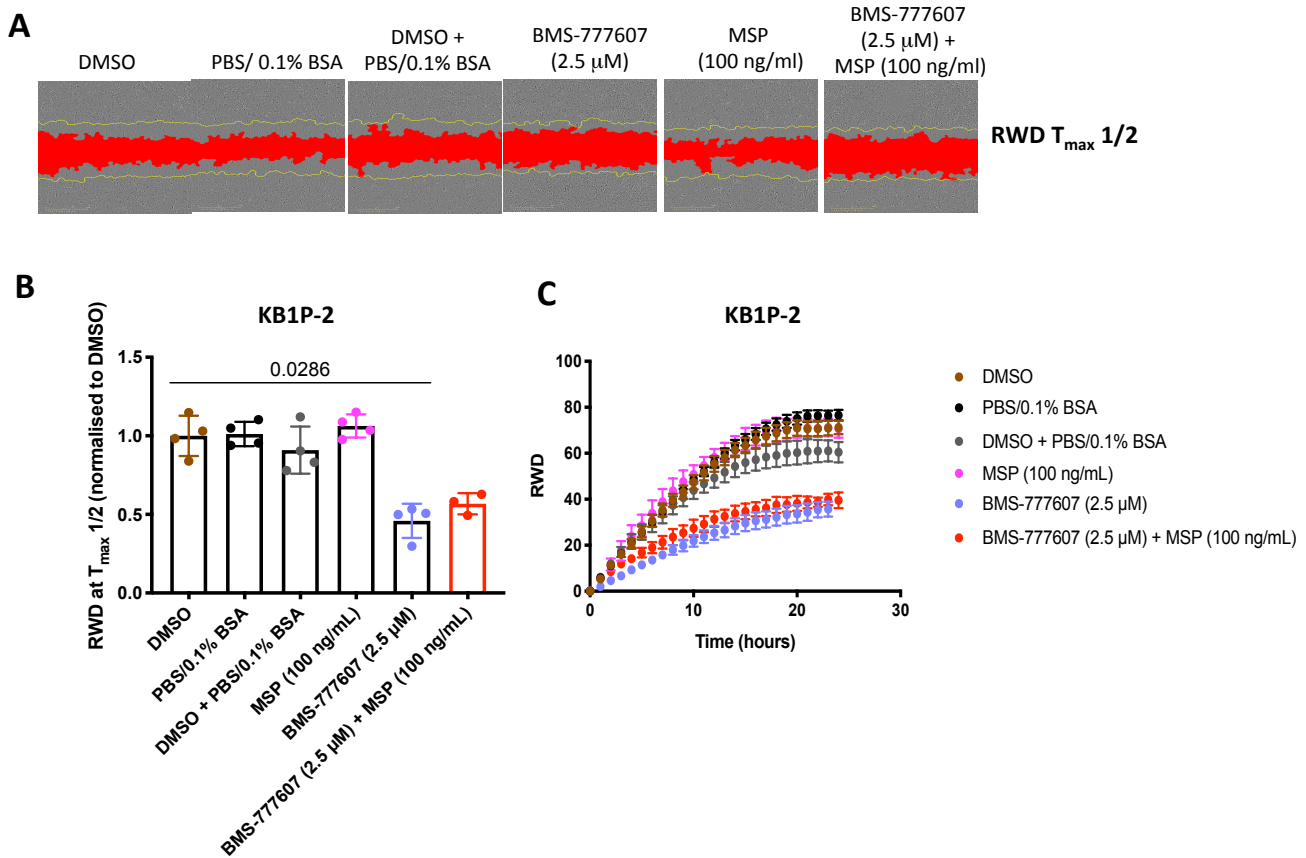


Figure 7. Inhibition of the RON-MSP axis reduces invasiveness in KB1P cells *in vitro*. (A) Representative image of relative wound density (RWD $T_{max} 1/2$) in KB1P tumour cell line. (B) RWD $T_{max} 1/2$ in KB1P cell line, DMSO control normalised. (C) RWD over time in KB1P cell line (Mann-Whitney test). Cells were allowed to attached overnight to form monolayers. Next, cells were wounded and treated with BMS-777607 (in DMSO), MSP (in PBS/0.1% BSA) or a combination, at the indication concentrations in low serum (0.2% FBS) conditions. Images are representative of at least three independent experiments.

3.7 The V γ 1 $\gamma\delta$ T cell subset is restricted to IFN γ -producing $\gamma\delta$ T cells and V γ 4 $\gamma\delta$ T cells expand in the presence of a mammary tumour

In the first part of this study we focused on the mammary tumour and aimed to elucidate the role of the RON-MSP axis in triple negative breast cancer metastasis. Next, we shifted our focus to the immune cells in the tumour microenvironment. We had assessed the importance of the $\gamma\delta$ T cell-IL-17-neutrophils axis in the KB1P and KP mammary tumour models. Moving forward, we aimed to elucidate the role of the IFN γ -producing $\gamma\delta$ T cells in breast cancer metastasis. To this end, we first evaluated their expression in wild type and tumour bearing mice. We collected lung and lymph nodes from KB1P mice at clinical endpoint and age matched the wild type control mice. We observed similar levels of IFN γ -producing $\gamma\delta$ T cells in KB1P and wild-type mice in the lung (figure 2A, 8) and the lymph nodes (figure 2A, 8). Next, we asked the question whether IFN γ -producing $\gamma\delta$ T cells have a T cell receptor chain (TCR) usage profile different from IL17-producing $\gamma\delta$ T cells with the aim of finding a target to specifically deplete the former. While these two subsets can be distinguished based on their CD27 expression [83], CD27 is also expressed on other T cells, rendering an anti-CD27 antibody unsuitable for this purpose. The data show a striking difference in expression of the V γ -chain of the T cell receptor between the two $\gamma\delta$ T cell subsets (figure 9A, 9B). IFN γ -producing $\gamma\delta$ T cells and $\gamma\delta$ T cells that do not express IFN γ or IL-17 predominantly express the V γ 1 variant of the TCR, at over 50%. In contrast, only 5% of the IL-17-producing $\gamma\delta$ T cells express V γ 1. The majority (80%) of IL-17-producing $\gamma\delta$ T cells express neither V γ 1 or V γ 4. The $\gamma\delta$ T cells in wild type mice had a similar TCR profile, implying that the presence of a mammary tumour does not change the $\gamma\delta$ T cell repertoire. Interestingly, in tumour bearing KB1P mice we observed overall expansion of V γ 4 $\gamma\delta$ T cells for all $\gamma\delta$ T cell subsets. To

conclude, the data demonstrate that expression of the V γ 1 chain is selective for IFN γ -producing $\gamma\delta$ T cells and is a promising target to study the function of these cells.

3.8 Anti-V γ 1 antibody selectively depletes IFN γ -producing $\gamma\delta$ T cells and decreases IFN γ production on CD3⁺ T cells

To test this hypothesis and to validate whether we could specifically deplete IFN γ -producing $\gamma\delta$ T cells, we used an anti-V γ 1 antibody. Preliminary data in wild type mice show a reduction of ~50% in (CD27⁺) IFN γ -producing $\gamma\delta$ T cells which is in line with previous findings that approximately 50% of the cells express V γ 1, which demonstrates high selectivity and effectiveness of the antibody. Surprisingly, we also observed a decrease in IFN γ production by CD3⁺ T cells. Thus, the data demonstrate that an anti-V γ 1 antibody is suitable to deplete IFN γ -producing $\gamma\delta$ T cells and that these cells may prime CD3⁺ T cells (i.e. CD8⁺ T cells) for their IFN γ production and their subsequent cytotoxic anti-tumour activity. For future experiments the drug tolerance of the mice to BMS-777607 was tested. Mice were treated for 5 consecutive days per week, for a total of 12 days. 100% of the mouse cohort tolerated the drug and no signs of a worsened animal health (e.g. 10% weight loss) were observed (data not shown).

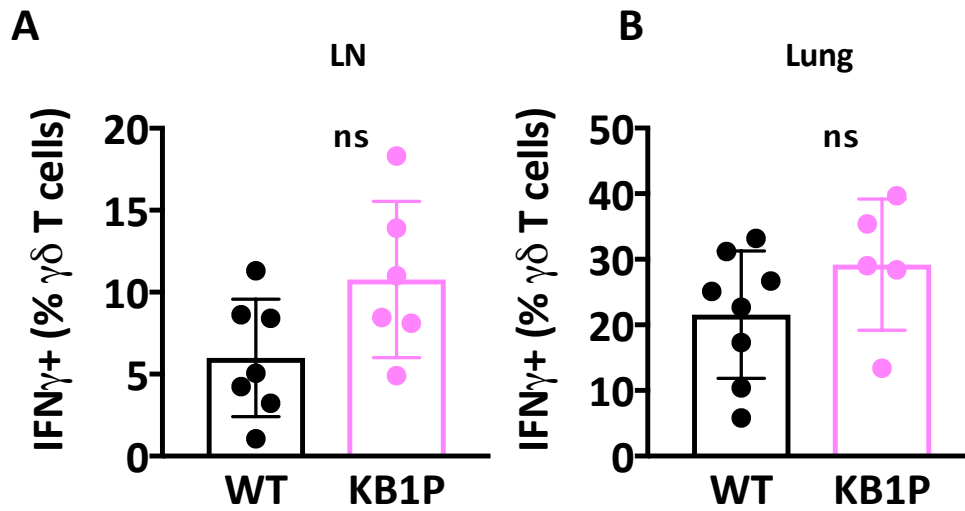


Figure 8. IFN γ -producing $\gamma\delta$ T cells in WT and KB1P mice. (A) IFN γ $\gamma\delta$ T cells in wild type and KB1P mice (LN: n = 7 WT, n = 6 KB1P; Lung: n = 8 WT, n = 5 KB1P; Mann-Whitney test). Lungs and lymph nodes were collected from mice at clinical endpoint. Lungs were digested with collagenase D and red blood cells were lysed. Remaining cells were collected and incubated with antibodies using a 10-colour T cell flow cytometry panel. B-lymphocytes (CD19) and epithelial cells (EpCAM) were gated out by means of a dump channel (APC-eFluor780). The percentages shown represent the frequency of cells relative to the parent gate. Immune cell populations are shown as proportion of the total amount of $\gamma\delta$ T cells. All data are mean (SD).

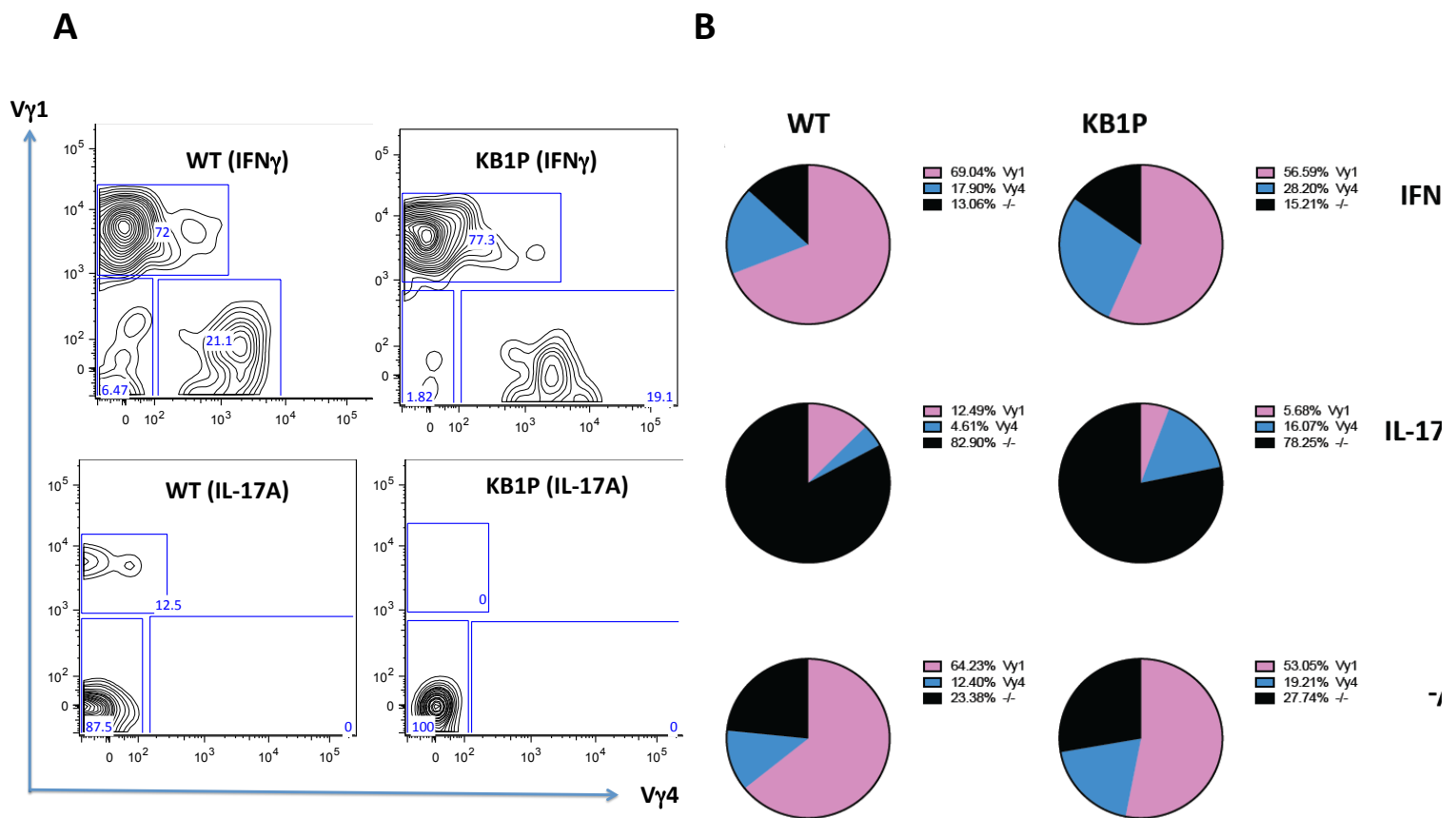


Figure 9. $\gamma\delta$ T cell repertoire in lungs of wild type and BRCA1-deficient mice. (A) Representative images of V γ 1-V γ 4 flow gate from IFN γ - $\gamma\delta$ T cell and IL-17A $\gamma\delta$ T cell parent gates, respectively. (B) V γ chain TCR usage of IFN γ -producing $\gamma\delta$ T cells, IL-17A producing $\gamma\delta$ T cells and IFN γ IL-17A \cdot $\gamma\delta$ T cells (IFN γ : KB1P, n = 5, WT, n = 4; IL-17A: KB1P, n = 4 WT, n = 4). Lungs were collected from mice at clinical endpoint. Lungs were digested with collagenase D and red blood cells were lysed. Remaining cells were collected and incubated with antibodies using a 10-colour T cell flow cytometry panel. B-lymphocytes (CD19) and epithelial cells (EpCAM) were gated out by means of a dump channel (APC-eFluor780). The percentages shown represent the frequency of cells relative to the parent gate.

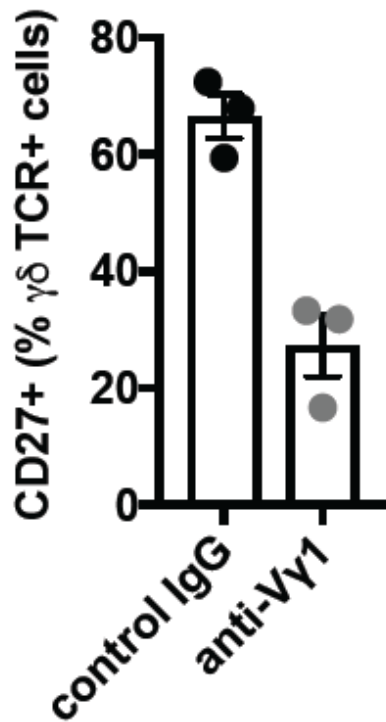
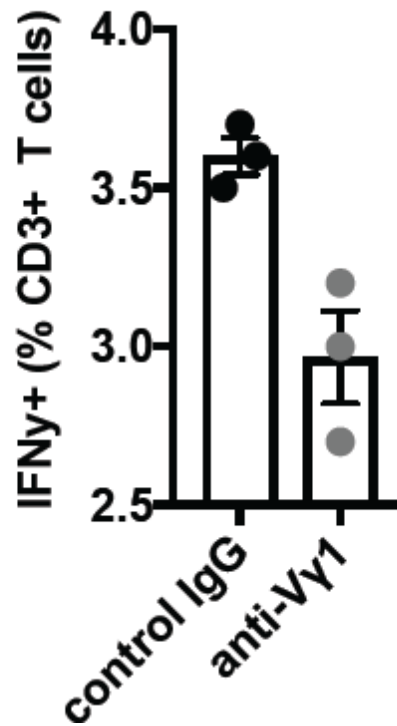
A**B**

Figure 10. Depletion of IFN γ -producing $\gamma\delta$ T cells reduces IFN γ expression on CD3+ T cells in lungs of wild type mice. (A) CD27⁺ expression on $\gamma\delta$ T cells. (B) IFN γ ⁺ expression on CD3⁺ T cells. Wild type mice were treated (IP) with anti-V γ 1 once a day for three consecutive days and sacrificed on the fourth day. Lungs were collected and digested with collagenase D and red blood cells were lysed. Remaining cells were collected and incubated with antibodies using a 10-colour T cell flow cytometry panel. B-lymphocytes (CD19) and epithelial cells (EpCAM) were gated out by means of a dump channel (APC-eFluor780). The percentages shown represent the frequency of cells relative to the parent gate.

Chapter IV. Discussion

Results from previous studies showed the importance of the $\gamma\delta$ T cell - IL-17 - neutrophil cascade in metastasis in a mouse model of lobular breast cancer (KEP). In this study, we show that this metastatic cascade is also important in KB1P mice, a mouse model of triple negative breast cancer. KB1P mice show an increase in IL-17-producing $\gamma\delta$ T cells and neutrophilia, suggesting that different types of breast cancer may have a similar mechanism involved in metastasis. The $\gamma\delta$ T cell - IL-17 - neutrophil cascade is induced by macrophage-mediated IL-1 β secretion from the mammary tumour microenvironment [58]. Thus, we were interested in the mechanism used by the macrophages to secrete IL-1 β to facilitate metastasis. More specifically, we investigated the RON-MSP axis and found that MSP is upregulated in KB1P mice. Interestingly, this does not correspond to a change in the phenotype of the macrophages in KB1P mammary tumours, nor an increase in macrophage abundance. A similar phenomenon was observed in a mouse model of liver disease (NASH). *Ldlr*^{-/-} mice treated with MSP showed an increase in proinflammatory cytokines, including IL-1 β , without a change in macrophage infiltration [84]. However, we cannot rule out that a deeper analysis, such as RNA-Seq, could show a macrophage phenotype specific to KB1P mice, as we characterised the macrophage population based on their MHCII-expression. However, as a result of our findings, we shifted our focus to the mammary tumour. Serum levels and immunohistochemistry data implied a dependence of the KB1P mammary tumour on the RON-MSP axis. Furthermore, other studies have shown that tumour cells can facilitate IL-1 β production in tumour-associated macrophages. For example, Jang *et al* used murine triple negative breast cancer line 4T1 and observed macrophage-mediated

IL-1 β production through CD44 *in vitro*. Moreover, orthotopic transplantation of 4T1 cells in mice resulted in tumour growth and lung metastases [85]. Thus, we made KB1P (and KP) primary tumour cells lines and took a pharmacological approach to elucidate the role of the RON-MSP axis *in vitro*. KB1P tumour cells were insensitive to treatment with BMS-777607. In contrast, BRCA1-positive KP tumour cells showed a significant reduction in cell viability and subsequent increased apoptosis upon treatment with BMS-777607. Given the knowledge that the KP mouse model shows an overexpression of cMET [77], this observation could be explained by the fact that treatment with the cMET/RON dual inhibitor BMS-777607, has a synergistic effect in the KP cell lines. Reduced invasiveness of KB1P tumour cells, not reversible by MSP, upon treatment with BMS-777607 implies the requirement of RON-MSP axis for the tumourigenic potential of the cancer cells. Other members of the lab have followed up on these findings and the data have given insight into the role of the RON-MSP axis in tumourigenesis *in vivo*. FVB/n mice transplanted with KB1P tumour fragments into the mammary gland showed a delay in primary tumour growth upon treatment with BMS-777607 as a result of a decrease in cell proliferation [86].

In addition to the RON-MSP axis, we investigated the role of IFN γ $\gamma\delta$ T cells in breast cancer metastasis. Although these cells are proposed to have anti-tumourigenic potential, their role in breast cancer metastasis remains elusive. Our results show a striking difference in the T-cell receptor repertoire in these IFN γ $\gamma\delta$ T cells compared to their IL-17-producing counterparts. The V γ 1 variant of the TCR is selective for the IFN γ -producing $\gamma\delta$ T cells, independently of the presence of a mammary tumour. Overall expansion of V γ 4 $\gamma\delta$ T cells in the mammary tumour microenvironment suggests that these may be favoured in the tumour

microenvironment, although this hypothesis will need to be investigated. We show that depletion with an anti-V γ 1 antibody selectively targets IFN γ -producing $\gamma\delta$ T cells. Additionally, the interesting observation that this also resulted in IFN γ production on CD3⁺ T cells implies that other T cells (i.e. CD8⁺ T cells) may require priming from IFN γ -producing $\gamma\delta$ T cells for their cytotoxic tumour-killing abilities. Consequently, we reason that neutrophils (through the $\gamma\delta$ T cell - IL-17 - neutrophil cascade) suppress IFN γ -producing $\gamma\delta$ T cells and that the mammary tumour activates this metastatic cascade through the RON-MSP axis, which it also requires for its own oncogenic potential.

Future experiments will focus on testing our hypotheses and metastatic cascade-working model in tumour-bearing mice (figure 11). Although several studies have suggested a role of the RON-MSP axis in metastasis, it is important to note that these studies were performed in MSP overexpressing cell lines derived from the *MMTV-PyMT* model or *MMTV*-driven *Mst1r* overexpressing genetically engineered mouse models. Compared to our KB1P model, the tumours of these models show less resemblance to human TBNC tumours on a histological level. Furthermore, the KB1P mice have increased endogenous levels of MSP, allowing for less artificial manipulation to perform *in vivo* experiments and a more representative simulation of TBNC progression as seen in patients.

We will use the metastasis model (as described in [60]) and use both a pharmacological approach and use various genetically engineered mouse models. For the pharmacological approach, KB1P tumour fragments will be transplanted in wild type syngeneic FVB/N mice. Next, using anti-Ly6G and anti-V γ 1 antibodies, and/or BMS777607, neutrophils, IFN γ $\gamma\delta$ T cells and the RON-MSP axis will be

inhibited, respectively, to study the function of each target in the metastatic cascade. Another way to study the RON-MSP axis would be to cross *K14-Cre* mice with homozygous Ron-floxed mice to generate mice with deletion of RON in epithelial cells and to transplant KB1P tumour fragments in these mice. We hypothesise that inhibition of RON will result in a decreased number of (lung) metastases and prolong survival after removal of the primary tumour. Using the same approach (i.e. transplanting KB1P tumour fragments), CD3DH mice can be used to determine whether IFN γ -producing $\gamma\delta$ T cells are required for CD8⁺ T cell activation. The phenotype of these mice has been thoroughly described [87]. Briefly, these mice lack IFN γ -producing $\gamma\delta$ T cells and show impairment in differentiation of V γ 6, but not V γ 4 IL-17⁺ $\gamma\delta$ T cells. In contrast, they exhibit normal numbers and phenotype of $\alpha\beta$ T cells (e.g. CD8⁺ T cells). Thus, we hypothesise that more lung metastases will be found in these CD3DH mice compared to control mice, as a result of the lack of CD8⁺ T cell activation by IFN γ -producing $\gamma\delta$ T cells. Additionally, using this model we can also investigate the role of V γ 4 IL-17⁺ $\gamma\delta$ T cells, as the impact of the expansion of this $\gamma\delta$ T cell subset in the tumour microenvironment is still unclear.

To conclude, using both pharmacological methods and exploit various genetically engineered mouse models to perform metastasis studies, we hope to be able to get more insight into the mechanism of breast cancer metastasis, focusing on both the mammary tumour and anti-tumourigenic IFN γ $\gamma\delta$ T cells in the tumour microenvironment. Ultimately, with this knowledge, the aim is to develop new combinatorial approaches targeting both cancer cells and immune cells to abrogate breast cancer metastasis.

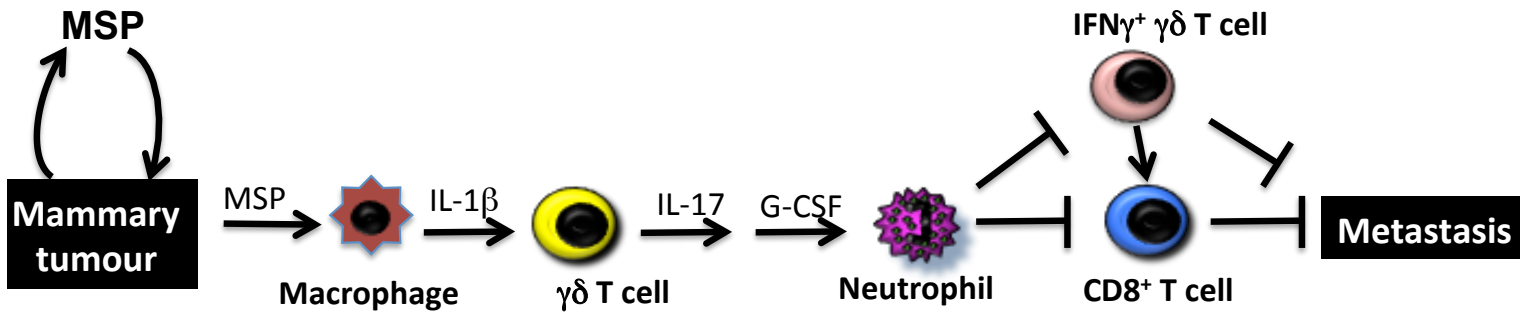


figure 11. Working model metastatic cascade. MSP is used by the mammary tumour for its oncogenic potential. In addition, through MSP, the mammary tumour stimulates IL-1 β secretion by macrophages to induce the $\gamma\delta$ T cell - IL-17 - neutrophil cascade, which inhibits CD8 $^+$ T cells and IFN γ δ T cells and results in metastasis. IFN γ $^+$ $\gamma\delta$ T cells also prime CD8 $^+$ T cells for their cytotoxic properties.

Chapter V. References

1. Bray, F., et al., *Global cancer statistics 2018: GLOBOCAN estimates of incidence and mortality worldwide for 36 cancers in 185 countries*. CA Cancer J Clin, 2018. **68**(6): p. 394-424.
2. Vallejos, C.S., et al., *Breast cancer classification according to immunohistochemistry markers: subtypes and association with clinicopathologic variables in a peruvian hospital database*. Clin Breast Cancer, 2010. **10**(4): p. 294-300.
3. Dai, X., et al., *Breast cancer intrinsic subtype classification, clinical use and future trends*. Am J Cancer Res, 2015. **5**(10): p. 2929-43.
4. Eroles, P., et al., *Molecular biology in breast cancer: intrinsic subtypes and signaling pathways*. Cancer Treat Rev, 2012. **38**(6): p. 698-707.
5. Rouzier, R., et al., *Breast cancer molecular subtypes respond differently to preoperative chemotherapy*. Clin Cancer Res, 2005. **11**(16): p. 5678-85.
6. Shagufta and I. Ahmad, *Tamoxifen a pioneering drug: An update on the therapeutic potential of tamoxifen derivatives*. Eur J Med Chem, 2018. **143**: p. 515-531.
7. Cheang, M.C., et al., *Ki67 index, HER2 status, and prognosis of patients with luminal B breast cancer*. J Natl Cancer Inst, 2009. **101**(10): p. 736-50.
8. Tran, B. and P.L. Bedard, *Luminal-B breast cancer and novel therapeutic targets*. Breast Cancer Res, 2011. **13**(6): p. 221.
9. Weigelt, B., et al., *Breast cancer molecular profiling with single sample predictors: a retrospective analysis*. Lancet Oncol, 2010. **11**(4): p. 339-49.
10. Avraham, R. and Y. Yarden, *Feedback regulation of EGFR signalling: decision making by early and delayed loops*. Nat Rev Mol Cell Biol, 2011. **12**(2): p. 104-17.
11. Hudis, C.A., *Trastuzumab--mechanism of action and use in clinical practice*. N Engl J Med, 2007. **357**(1): p. 39-51.
12. Bertucci, F., et al., *How basal are triple-negative breast cancers?* Int J Cancer, 2008. **123**(1): p. 236-40.
13. Badve, S., et al., *Basal-like and triple-negative breast cancers: a critical review with an emphasis on the implications for pathologists and oncologists*. Mod Pathol, 2011. **24**(2): p. 157-67.
14. Alluri, P. and L.A. Newman, *Basal-like and triple-negative breast cancers: searching for positives among many negatives*. Surg Oncol Clin N Am, 2014. **23**(3): p. 567-77.
15. Leidy, J., A. Khan, and D. Kandil, *Basal-like breast cancer: update on clinicopathologic, immunohistochemical, and molecular features*. Arch Pathol Lab Med, 2014. **138**(1): p. 37-43.
16. Hill, S.J., et al., *BRCA1 pathway function in basal-like breast cancer cells*. Mol Cell Biol, 2014. **34**(20): p. 3828-42.
17. Couch, F.J., K.L. Nathanson, and K. Offit, *Two decades after BRCA: setting paradigms in personalized cancer care and prevention*. Science, 2014. **343**(6178): p. 1466-70.

18. Prakash, R., et al., *Homologous recombination and human health: the roles of BRCA1, BRCA2, and associated proteins*. Cold Spring Harb Perspect Biol, 2015. **7**(4): p. a016600.
19. Lord, C.J. and A. Ashworth, *The DNA damage response and cancer therapy*. Nature, 2012. **481**(7381): p. 287-94.
20. Lord, C.J. and A. Ashworth, *BRCAness revisited*. Nat Rev Cancer, 2016. **16**(2): p. 110-20.
21. Yarchoan, M., et al., *Olaparib in combination with irinotecan, cisplatin, and mitomycin C in patients with advanced pancreatic cancer*. Oncotarget, 2017. **8**(27): p. 44073-44081.
22. Dhawan, M. and C.J. Ryan, *BRCAness and prostate cancer: diagnostic and therapeutic considerations*. Prostate Cancer Prostatic Dis, 2018. **21**(4): p. 488-498.
23. Surveillance, E., and End Results Program (SEER). *Cancer Stat Facts: Female Breast Cancer*. [cited 2018 01 May].
24. Redig, A.J. and S.S. McAllister, *Breast cancer as a systemic disease: a view of metastasis*. J Intern Med, 2013. **274**(2): p. 113-26.
25. Jin, X. and P. Mu, *Targeting Breast Cancer Metastasis*. Breast Cancer (Auckl), 2015. **9**(Suppl 1): p. 23-34.
26. Hunter, K.W., N.P. Crawford, and J. Alsarraj, *Mechanisms of metastasis*. Breast Cancer Res, 2008. **10 Suppl 1**: p. S2.
27. Fidler, I.J., *The pathogenesis of cancer metastasis: the 'seed and soil' hypothesis revisited*. Nat Rev Cancer, 2003. **3**(6): p. 453-8.
28. Hanahan, D. and R.A. Weinberg, *Hallmarks of cancer: the next generation*. Cell, 2011. **144**(5): p. 646-74.
29. Kitamura, T., B.Z. Qian, and J.W. Pollard, *Immune cell promotion of metastasis*. Nat Rev Immunol, 2015. **15**(2): p. 73-86.
30. Fleming, C., et al., *gammadelta T Cells: Unexpected Regulators of Cancer Development and Progression*. Trends Cancer, 2017. **3**(8): p. 561-570.
31. Mantovani, A., et al., *Tumour-associated macrophages as treatment targets in oncology*. Nat Rev Clin Oncol, 2017. **14**(7): p. 399-416.
32. Pollard, J.W., *Macrophages define the invasive microenvironment in breast cancer*. J Leukoc Biol, 2008. **84**(3): p. 623-30.
33. Yang, M., et al., *Stromal Infiltration of Tumor-Associated Macrophages Conferring Poor Prognosis of Patients with Basal-Like Breast Carcinoma*. J Cancer, 2018. **9**(13): p. 2308-2316.
34. Mantovani, A., et al., *Macrophage polarization: tumor-associated macrophages as a paradigm for polarized M2 mononuclear phagocytes*. Trends Immunol, 2002. **23**(11): p. 549-55.
35. Mosser, D.M. and J.P. Edwards, *Exploring the full spectrum of macrophage activation*. Nat Rev Immunol, 2008. **8**(12): p. 958-69.
36. Aras, S. and M.R. Zaidi, *TAMEless traitors: macrophages in cancer progression and metastasis*. Br J Cancer, 2017. **117**(11): p. 1583-1591.
37. Lin, E.Y. and J.W. Pollard, *Tumor-associated macrophages press the angiogenic switch in breast cancer*. Cancer Res, 2007. **67**(11): p. 5064-6.
38. Lin, E.Y., et al., *Macrophages regulate the angiogenic switch in a mouse model of breast cancer*. Cancer Res, 2006. **66**(23): p. 11238-46.
39. Movahedi, K., et al., *Different tumor microenvironments contain functionally distinct subsets of macrophages derived from Ly6C(high) monocytes*. Cancer Res, 2010. **70**(14): p. 5728-39.

40. Noy, R. and J.W. Pollard, *Tumor-associated macrophages: from mechanisms to therapy*. *Immunity*, 2014. **41**(1): p. 49-61.
41. Qian, B.Z., et al., *FLT1 signaling in metastasis-associated macrophages activates an inflammatory signature that promotes breast cancer metastasis*. *J Exp Med*, 2015. **212**(9): p. 1433-48.
42. Xu, M., et al., *Intratumoral Delivery of IL-21 Overcomes Anti-Her2/Neu Resistance through Shifting Tumor-Associated Macrophages from M2 to M1 Phenotype*. *J Immunol*, 2015. **194**(10): p. 4997-5006.
43. DeNardo, D.G., et al., *Leukocyte complexity predicts breast cancer survival and functionally regulates response to chemotherapy*. *Cancer Discov*, 2011. **1**(1): p. 54-67.
44. Leiding, J.W., *Neutrophil Evolution and Their Diseases in Humans*. *Front Immunol*, 2017. **8**: p. 1009.
45. Templeton, A.J., et al., *Prognostic role of neutrophil-to-lymphocyte ratio in solid tumors: a systematic review and meta-analysis*. *J Natl Cancer Inst*, 2014. **106**(6): p. dju124.
46. Gentles, A.J., et al., *The prognostic landscape of genes and infiltrating immune cells across human cancers*. *Nat Med*, 2015. **21**(8): p. 938-945.
47. Coffelt, S.B., M.D. Wellenstein, and K.E. de Visser, *Neutrophils in cancer: neutral no more*. *Nat Rev Cancer*, 2016. **16**(7): p. 431-46.
48. Vantourout, P. and A. Hayday, *Six-of-the-best: unique contributions of gammadelta T cells to immunology*. *Nat Rev Immunol*, 2013. **13**(2): p. 88-100.
49. Bonneville, M., et al., *Chicago 2014--30 years of gammadelta T cells*. *Cell Immunol*, 2015. **296**(1): p. 3-9.
50. Lafont, V., et al., *Plasticity of gammadelta T Cells: Impact on the Anti-Tumor Response*. *Front Immunol*, 2014. **5**: p. 622.
51. Hayday, A.C., *Gammadelta T cells and the lymphoid stress-surveillance response*. *Immunity*, 2009. **31**(2): p. 184-96.
52. Hayday, A.C., *[gamma][delta] cells: a right time and a right place for a conserved third way of protection*. *Annu Rev Immunol*, 2000. **18**: p. 975-1026.
53. Bonneville, M., R.L. O'Brien, and W.K. Born, *Gammadelta T cell effector functions: a blend of innate programming and acquired plasticity*. *Nat Rev Immunol*, 2010. **10**(7): p. 467-78.
54. Carding, S.R. and P.J. Egan, *Gammadelta T cells: functional plasticity and heterogeneity*. *Nat Rev Immunol*, 2002. **2**(5): p. 336-45.
55. O'Brien, R.L. and W.K. Born, *gammadelta T cell subsets: a link between TCR and function?* *Semin Immunol*, 2010. **22**(4): p. 193-8.
56. Ribot, J.C. and B. Silva-Santos, *Differentiation and activation of gammadelta T Lymphocytes: Focus on CD27 and CD28 costimulatory receptors*. *Adv Exp Med Biol*, 2013. **785**: p. 95-105.
57. Silva-Santos, B., *Promoting angiogenesis within the tumor microenvironment: the secret life of murine lymphoid IL-17-producing gammadelta T cells*. *Eur J Immunol*, 2010. **40**(7): p. 1873-6.
58. Coffelt, S.B., et al., *IL-17-producing gammadelta T cells and neutrophils conspire to promote breast cancer metastasis*. *Nature*, 2015. **522**(7556): p. 345-348.
59. Derksen, P.W., et al., *Somatic inactivation of E-cadherin and p53 in mice leads to metastatic lobular mammary carcinoma through induction of anoikis resistance and angiogenesis*. *Cancer Cell*, 2006. **10**(5): p. 437-49.

60. Doornebal, C.W., et al., *A preclinical mouse model of invasive lobular breast cancer metastasis*. *Cancer Res*, 2013. **73**(1): p. 353-63.
61. Chen, W.C., et al., *Interleukin-17-producing cell infiltration in the breast cancer tumour microenvironment is a poor prognostic factor*. *Histopathology*, 2013. **63**(2): p. 225-33.
62. Qian, B.Z. and J.W. Pollard, *Macrophage diversity enhances tumor progression and metastasis*. *Cell*, 2010. **141**(1): p. 39-51.
63. Ma, C., et al., *Tumor-infiltrating gammadelta T lymphocytes predict clinical outcome in human breast cancer*. *J Immunol*, 2012. **189**(10): p. 5029-36.
64. Liu, X., et al., *Somatic loss of BRCA1 and p53 in mice induces mammary tumors with features of human BRCA1-mutated basal-like breast cancer*. *Proc Natl Acad Sci U S A*, 2007. **104**(29): p. 12111-6.
65. Butti, R., et al., *Receptor tyrosine kinases (RTKs) in breast cancer: signaling, therapeutic implications and challenges*. *Mol Cancer*, 2018. **17**(1): p. 34.
66. Wagh, P.K., B.E. Peace, and S.E. Waltz, *Met-related receptor tyrosine kinase Ron in tumor growth and metastasis*. *Adv Cancer Res*, 2008. **100**: p. 1-33.
67. Bardella, C., et al., *Truncated RON tyrosine kinase drives tumor cell progression and abrogates cell-cell adhesion through E-cadherin transcriptional repression*. *Cancer Res*, 2004. **64**(15): p. 5154-61.
68. Yao, H.P., et al., *MSP-RON signalling in cancer: pathogenesis and therapeutic potential*. *Nat Rev Cancer*, 2013. **13**(7): p. 466-81.
69. Faham, N. and A.L. Welm, *RON signaling is a key mediator of tumor progression in many human cancers*. *Cold Spring Harb Symp Quant Biol*, 2017. **81**.
70. O'Toole, J.M., et al., *Therapeutic implications of a human neutralizing antibody to the macrophage-stimulating protein receptor tyrosine kinase (RON), a c-MET family member*. *Cancer Res*, 2006. **66**(18): p. 9162-70.
71. Wang, M.H., et al., *Altered expression of the RON receptor tyrosine kinase in various epithelial cancers and its contribution to tumorigenic phenotypes in thyroid cancer cells*. *J Pathol*, 2007. **213**(4): p. 402-11.
72. Maggiora, P., et al., *Overexpression of the RON gene in human breast carcinoma*. *Oncogene*, 1998. **16**(22): p. 2927-33.
73. Welm, A.L., et al., *The macrophage-stimulating protein pathway promotes metastasis in a mouse model for breast cancer and predicts poor prognosis in humans*. *Proc Natl Acad Sci U S A*, 2007. **104**(18): p. 7570-5.
74. Liu, X., et al., *Short-Form Ron Promotes Spontaneous Breast Cancer Metastasis through Interaction with Phosphoinositide 3-Kinase*. *Genes Cancer*, 2011. **2**(7): p. 753-62.
75. Eyob, H., et al., *Inhibition of ron kinase blocks conversion of micrometastases to overt metastases by boosting antitumor immunity*. *Cancer Discov*, 2013. **3**(7): p. 751-60.
76. Gurusamy, D., et al., *Myeloid-specific expression of Ron receptor kinase promotes prostate tumor growth*. *Cancer Res*, 2013. **73**(6): p. 1752-63.
77. Liu, H., et al., *Identifying and Targeting Sporadic Oncogenic Genetic Aberrations in Mouse Models of Triple-Negative Breast Cancer*. *Cancer Discov*, 2018. **8**(3): p. 354-369.
78. Azab, B., et al., *Usefulness of the neutrophil-to-lymphocyte ratio in predicting short- and long-term mortality in breast cancer patients*. *Ann Surg Oncol*, 2012. **19**(1): p. 217-24.
79. Gao, Y., et al., *Gamma delta T cells provide an early source of interferon gamma in tumor immunity*. *J Exp Med*, 2003. **198**(3): p. 433-42.

80. Girardi, M., et al., *Regulation of cutaneous malignancy by gammadelta T cells*. Science, 2001. **294**(5542): p. 605-9.
81. Liu, Z., et al., *Protective immunosurveillance and therapeutic antitumor activity of gammadelta T cells demonstrated in a mouse model of prostate cancer*. J Immunol, 2008. **180**(9): p. 6044-53.
82. Van Overmeire, E., et al., *Mechanisms driving macrophage diversity and specialization in distinct tumor microenvironments and parallels with other tissues*. Front Immunol, 2014. **5**: p. 127.
83. Ribot, J.C., et al., *CD27 is a thymic determinant of the balance between interferon-gamma- and interleukin 17-producing gammadelta T cell subsets*. Nat Immunol, 2009. **10**(4): p. 427-36.
84. Li, J., et al., *Macrophage Stimulating Protein Enhances Hepatic Inflammation in a NASH Model*. PLoS One, 2016. **11**(9): p. e0163843.
85. Jang, J.H., et al., *Breast Cancer Cell-Derived Soluble CD44 Promotes Tumor Progression by Triggering Macrophage IL1beta Production*. Cancer Res, 2020. **80**(6): p. 1342-1356.
86. Millar, R., et al., *The MSP-ROn axis stimulates cancer cell growth in models of triple negative breast cancer*. Mol Oncol, 2020. **14**(8): p. 1868-1880.
87. Munoz-Ruiz, M., et al., *TCR signal strength controls thymic differentiation of discrete proinflammatory gammadelta T cell subsets*. Nat Immunol, 2016. **17**(6): p. 721-727.